CHARGE SCHEDULING AND ROUTE PLANNING OF COMMERCIAL ELECTRIC VEHICLES BY CONSIDERING THE EFFECT OF BATTERY DEGRADATION

by

Raci Berk İslim

Submitted to the Graduate School of Engineering and Natural Sciences

in partial fulfilment of

the requirements for the degree of Master of Sciences

Sabancı University

July 2022

ABSTRACT

CHARGE SCHEDULING AND ROUTE PLANNING OF COMMERCIAL ELECTRIC VEHICLES BY CONSIDERING THE EFFECT OF BATTERY DEGRADATION

Raci Berk İslim

Industrial Engineering, Master's Thesis, July 2022

Thesis Supervisor: Prof. Dr. Bülent Çatay

Keywords: electric vehicle, vehicle routing problem, traveling salesman problem, time windows, battery degradation, matheuristic, charge planning

Battery is a critical component of electric vehicles (EVs) due to its limited useful economic life and high production cost. Hence, better recharging and discharging practices through coordinated and improved route planning decisions may be a remedy for maintaining good battery health and avoiding fast degradation. In this study, we investigate the effect of considering the battery degradation-related cost on the route and charge planning of commercial EVs within the context of the Electric Traveling Salesman Problem with Time Windows (ETSPTW) and Electric Vehicle Routing Problem with Time Windows (EVRPTW). First, we extend the mathematical programming formulation of the ETSPTW, where the objective function minimizes the costs associated with battery degradation and energy consumption. Next, we develop a Variable Neighborhood Search (VNS) based matheuristic enhanced with an exact solver employed for the post-optimization of heuristic solutions. Our matheuristic also includes a new mechanism designed specific to our problem. Then, we perform computational experiments using benchmark instances from the literature, and our results demonstrate that the proposed matheuristic achieves good quality solutions within reasonable computational time. We also extend the mathematical model of the EVRPTW by considering the battery degradation and conduct a computational study by solving small-size instances from the

literature on a commercial solver. Our results in both problem settings show that incorporating battery degradation in the problem may yield significant changes in the route plans. On the one hand, it offers a potential for substantial reduction in operational costs compared to the solutions obtained by minimizing energy consumption only. On the other hand, it leads to more frequent recharges en route, which brings in additional operational hurdles.

ÖZET

BATARYA YIPRANMASININ ETKİSİ GÖZ ÖNÜNDE BULUNDULARARAK ELEKTRİKLİ TİCARİ ARAÇLARIN ŞARJ VE ROTA PLANLANMASI

Raci Berk İslim

Endüstri Mühendisliği, Yüksek Lisans Tezi, Temmuz 2022

Tez Danışmanı: Prof. Dr. Bülent Çatay

Anahtar Kelimeler: elektrikli araç, araç rotalama problemi, gezgin satıcı problemi, zaman penceresi, batarya yıpranması, mat-sezgisel, şarj planlaması

Batarya, kısıtlı kullanım ömrü ve yüksek ürettim maliyetlerinden dolayı elektrikli araçların (EA) en önemli bileşenlerinden biridir. Bu sebeple eş güdümlü ve gelişmiş rota planlamaları ile beraber uygulanacak iyileştirilmiş şarj ve deşarj uygulamaları batarya sağlığını korumak ve bataryanın hızlı yıpranmasını önlemek için bir çözüm olabilir. Bu çalışmada Zaman Pencereli Elektrikli Gezgin Satıcı Problemi (ZPEGSP) ve Zaman Pencereli Elektrikli Araç Rotalama Problemi (ZPEARP) kapsamında batarya yıpranmasına ilişkin maliyetlerin ticari EA'ların rota ve şarj planlamaları sırasında dikkate alınmasının etkisini inceliyoruz. İlk olarak ZPEGSP'nin matematiksel programlama formülasyonunu amaç fonksiyonunun batarya yıpranması ve enerji tüketimiyle ilişkilendirilen maliyetleri en küçükleyeceği şekilde genişletiyoruz. Daha sonrasında, sezgisel sonuçların son optimizasyonu için kullanılan kesin çözücüyle geliştirilmiş Değişken Komşuluk Arama (DKA) tabanlı bir mat-sezgisel geliştiriyoruz. Mat-sezgiselimiz problemimize özgü tasarlanan bir mekanizma da içermektedir. Akabinde, literatürdeki problem örneklerini kullanarak sayısal deneyler gerçekleştiriyoruz ve elde ettiğimiz sonuçlar önerdiğimiz mat-sezgiselin iyi kalitede çözümlere makul çalışma süreleri içerisinde ulaştığını gösterir. Ayrıca, batarya yıpranmasını dikkate alarak ZPEARP'nin matematiksel modelini de genişletiyoruz ve literatürdeki küçük boyutlu örnekleri bu model ile çözerek bir deney gerçekleştiriyoruz. İki problem ortamında da elde ettiğimiz sonuçlar, batarya yıpranmasını probleme dahil

etmenin rota planlamalarında dikkate değer değişikliklere sebep olabileceğini gösterir. Bir yandan sadece enerji sarfiyatının en küçüklendiği durumda elde edilen çözümlere kıyasla işletme maliyetlerinde önemli bir azalma imkanı sunar. Diğer yandan, rota boyunca daha sık şarj yapılmasına yol açar ve bu da ek operasyonel engeller getirir.

ACKNOWLEDGEMENTS

First and foremost, I would like to thank my thesis advisor Prof. Dr. Bülent Çatay for his support, sincerity and endless patience. He always guided me with his immense knowledge and research experience even the times our study gets stuck. I have learned many things from him, and he became one of the few people in my life whose opinion I value. It was a real fortune and honor to work with him.

I would like to thank my jury members Merve Keskin Özel and Sina Rastani for their valuable comments and feedback.

A special thanks to the organization of Sabancı University for creating a free environment. I had an opportunity to take lessons from very valuable academicians and meet highly qualified graduate students. I feel privileged for being a student and employee of the university.

I am very thankful to my mother Emel and brother Buğra for their support. They always encouraged me to pursue an academic career. I am sure that my father would be proud of me if he was able to see what I have accomplished.

I would like to thank my girlfriend Hazel for her understanding and continuous support. She helped me improve my programming skills. She knows the progress of this study from very the beginning, and I am grateful to her for being able to share these kinds of experiences.

Finally, I acknowledge that this study was partially supported by The Scientific and Technical Research Council of Turkey (TÜBİTAK) through Grant # 118M412.

to my mother

TABLE OF CONTENTS

LIST OF TABLES

LIST OF FIGURES

LIST OF ABBREVIATIONS

GHG: Greenhouse Gas ..... …

BEV: Battery Electric Vehicle..... …

LSP: Logistics Service Provider……...

EV: Electric Vehicle ..... …

AFV: Alternative Fuel Vehicle..... …

LNG: Liquefied Natural Gas……..

CNG: Compressed Natural Gas……

ICEV: Internal Combustion Engine Vehicle ..... …

HEV: Hybrid Electric Vehicle……..

FCEV: Fuel Cell Electric Vehicle……

VRP: Vehicle Routing Problem..... …..

ETSPTW: Electric Traveling Salesman Problem with Time Windows……

EVRPTW: Electric Vehicle Routing Problem with Time Windows..... …….

ETSPTW-BD: Electric Traveling Salesman Problem with Time Windows and Battery Degradation……..

EVRPTW-BD: Electric Vehicle Routing Problem with Time Windows and Battery Degradation……..

VNS: Variable Neighborhood Search……..

OR: Operations Research……....

GVRP: Green Vehicle Routing Problem.....

HEVTSP: Hybrid Electric Vehicle Traveling Salesman Problem……

HEVTSPTW: Hybrid Electric Vehicle Traveling Salesman Problem with Time Windows……..

LRP: Location Routing Problem…….....

SOC: State of Charge..... ….

EFV: Electric Freight Vehicle…….....

DOD: Depth of Discharge……

ACC: Achievable Cycle Count……

kWh: Kilowatt-Hour……

SOH: State of Health……

WC: Wear Cost……

LS: Local-Search…….

FTVCP: Fixed-Tour Vehicle-Charging Problem…….....

FRVCP: Fixed-Route Vehicle-Charging Problem…….....

OFV: Objective Function Value……...

BKS: Best-Known Solution…….

BF: Best-Found……

ALNS: Adaptive Large Neighborhood Search…….

1. INTRODUCTION

Transportation sector is responsible for about 25% of overall CO_2 emissions which is one of the most widespread greenhouse gases (GHG). Road transportation accounts for 75% of this transportation related emission (International Energy Agency, 2020). More specifically, with the substantial surge in e-commerce activities through B2C and C2C channels, last mile deliveries performed by logistics companies have excessively increased in the last decade, and this trend is expected to continue in the future (McKinsey, 2016). However, last mile delivery is one of the most unsustainable operations covered by logistics service providers (LSPs) (Jiang et al., 2019). Hence, many governments started to take initiatives and set regulations, such as monetary incentives for electric vehicle (EV) purchases and issuing directives to increase the number of recharging infrastructures and improve electrical networks, to mitigate the adverse environmental effects of transportation activities.

The initiatives taken by governments have led companies and government agencies to consider alternative fuel vehicles (AFVs), such as biodiesel-, LNG-, CNG-, electric- and hydrogen-powered vehicles, as substitutes for internal combustion engine vehicles (ICEVs) (Keskin and Çatay, 2018). Furthermore, battery electric vehicles (BEVs), hybrid electric vehicles (HEVs) and fuel cell electric vehicles (FCEVs) are generic types of EVs (Çatay and Keskin, 2017). In this thesis, we only deal with commercial BEVs, and will refer to them as EVs.

EVs have been one of the most attention-grabbing alternatives among such AFVs due to their certain advantages over ICEVs: (i) they do not create GHG in inner-city; (ii) the zero-emission objective can be reached if the energy used for recharging comes fully from renewable energy sources; (iii) their noise in traffic is negligible; (iv) fewer maintenance

activities are needed; and (v) they are more efficient at low speeds (Schiffer et al., 2016; Pelletier et al., 2016). These advantages indicate that EV usage in urban logistics is more favorable than ICEV usage. On the other hand, EVs have significant drawbacks compared to ICEVs: (i) their driving range is strictly limited; (ii) the recharging time of batteries is excessively long; and (iii) public charging stations are not widely available in inner cities and rural locations.

One of the most important aspects of last mile problems is the route optimization of delivery vehicles, i.e. the vehicle routing problem (VRP) (Deutsch and Golany, 2018). The LSPs are in the phase of renewing their fleets by acquiring EVs to use these vehicles in the last mile deliveries. On the other hand, EVs have significantly fewer components than ICEVs (Wolff et al., 2020), and the battery constitutes the major component in the total cost of ownership. (Fries et al., 2017). For this reason, battery utilization should be accounted for during making not only strategic but also operational decisions. However, this makes the routing problem even more complex.

In this study, we deal with the electric traveling salesman problem with time windows (ETSPTW) and electric VRP with time windows (EVRPTW). We aim to examine the influence of battery degradation (wear) cost on both route and charge plans of EVs that are operated by logistics companies. To the best of our knowledge, this constitutes the first study that attempts to make routing and charge planning decisions simultaneously in the presence of time windows restrictions for the large-size problem instances by taking into account the cost associated with battery degradation. Hence, the contributions of this study are threefold: (i) we extend the mathematical models of the ETSPTW and EVRPTW by incorporating the impact of battery degradation in the objective function and constraint set, and refer to these problems as ETSPTW and battery degradation (ETSPTW-BD) and EVRPTW and battery degradation (EVRPTW-BD), respectively; (ii) we propose a variable neighborhood search (VNS)-based matheuristic approach that benefits from an exact solver to enhance the charging-related decisions; and (iii) we demonstrate the impact of battery degradation on route planning decisions and costs.

The remainder of this thesis is organized as follows: Chapter 2 reviews the related literature. We provide the technical background on battery degradation and a formulation for battery wear cost in Chapter 3. We present mathematical formulation of the ETSPTW-BD in Chapter 4. We propose a matheuristic approach, called MatHeur, to solve the

ETSPTW-BD in Chapter 5. Chapter 6 presents the computational study to validate the performance of MatHeur and provide managerial insights by using benchmark instances from the literature. In Chapter 7, we introduce the EVRPTW-BD, formulate its mathematical model, and solve small-size instances from the literature by using a commercial solver. Finally, Chapter 8 provides concluding remarks and directions for future research.

2. LITERATURE REVIEW

The TSP and VRP are two of the oldest combinatorial optimization problems that have been studied the most in the Operations Research (OR) literature. This chapter reviews the TSP and VRP literature by focusing on the utilization of AFVs, EVs in particular, in the delivery operations and examine the studies where the battery degradation is considered in strategic-tactical and operational decision-making.

AFVs have been considered within the context of the TSP by Doppstadt et al. (2016) who introduced the hybrid electric vehicle TSP (HEVTSP) and extended it to the HEVTSP with time windows (HEVTSPTW) in Doppstadt et al. (2020). In these studies, they defined several arcs between each pair of nodes, where each arc corresponds to the trip using a different driving mode such as pure combustion and pure electric modes. Roberti and Wen (2016) introduced the ETSPTW using an EV for delivery operations in an urban area. They presented the mathematical model of the problem and developed a heuristic algorithm to solve it. The ETSPTW includes one extra limitation that recharging visits might take a longer time when compared to the refueling of other types of AFVs. Küçükoğlu et al. (2019) considered different charging rates at each customer location for recharging the battery in the scope of ETSPTW.

Erdoğan and Miller-Hooks (2012) introduced Green VRP (GVRP) which considers a fleet of AFVs. Since the AFVs have a limited driving range, they may need to refuel along their routes, and this adds further complexity to the problem. The EVPRPTW was proposed by Schneider et al. (2014), which is a special case of GVRP where the fleet consists of EVs. After this study, EVRP literature has been enriched on several aspects as follows: Keskin and Çatay (2016) extended the EVRPTW by allowing partial recharges

and designed an adaptive large neighborhood search algorithm (ALNS) to solve the problem. The effect of different charging technologies on the route plans was also investigated in the literature. (Felipe et al., 2014; Keskin and Çatay, 2018). Furthermore, Montoya et al. (2017) introduced nonlinear charging functions into the problem. The location routing problem (LRP) was extended by locating charging stations (Schiffer and Walther, 2017) and battery swapping stations (Yang and Sun, 2015; Hof et al., 2017) besides the routing decisions. Time-dependent travel times (Lu et al., 2020; Wang et al., 2020), waiting times at recharging stations (Keskin et al., 2019, Keskin et al. 2021) and electricity prices (Lin et al., 2021) were also considered in the EVRPTW literature. Energy consumption in EVs is influenced by internal and external factors, and the effect of road gradient and travel speed (Goeke and Schneider, 2015), ambient temperature (Rastani et al., 2019) and load of the vehicle (Kancharla and Ramaduari, 2020; Rastani and Çatay, 2021) on the route plans of EVs were also investigated. Flexible time windows (Taş, 2021) and alternative delivery locations (Sadati et al., 2022) were also studied in the literature. The reader may refer to Erdelić and Carić (2019) and Küçükoğlu et al. (2021) for other EVRP variants and solution procedures developed to solve it.

The literature generally has looked upon strategic-tactical decisions regarding EVs in terms of fixed costs of EV purchases, battery replacements and capacity loss of the batteries in the long run. Feng and Figliozzi (2013) took into account the purchase cost of EVs and battery replacements in a multi-period setting. However, the influence of the fleet composition on the routes was not considered in their study. Goeke and Schneider (2015) also considered battery replacement cost in the objective function of their mathematical model. Nonetheless, no battery degradation mechanism was incorporated into the model. Schiffer et al. (2021) established integrated planning to achieve both strategic and operational decisions for EV fleets. Although they considered battery degradation in terms of capacity loss, their resulting routes were not affected by this degradation mechanism. Xu et al. (2021) devised an on-demand charging strategy by considering battery degradation during they decide on the fleet size of a carsharing service provider. Even if their consideration of battery degradation has effects on tactical and operational decisions, this study does not contain any routing perspective. Zhang et al. (2021) demonstrated that a significant decrease in the lifecycle cost of the electric bus fleet and an increase in the battery lifetime of buses is attainable if battery aging is considered during charging and discharging cycles. However, finding the routes of these

buses was not discussed in this study. Guo et al. (2022) considered the battery degradation in the context of location routing problem (LRP). Even if the LRP literature has well-known problem instances, they did not test and benchmark their algorithm by using these instances. Furthermore, their problem instances do not include time window restrictions which are highly observed in the industrial applications and make harder to solve the EVRP. Moreover, they did not give any insight into changes in the routes.

In the context of operational decisions, battery degradation has been mostly considered in deciding the charge schedule of the EVs. Sassi et al. (2014) set bounds to the energy level in the battery during the routing of the EVs based on the assumption that batteries degrade faster at the extreme state of charge (SOC) values. Nevertheless, they neither utilized a sophisticated degradation mechanism in their model nor analyzed how much the resulting routes are sensitive to that bounds. This limit was included as a constraint in their model and has no effect on the objective function. Barco et al. (2017) followed a phase-by-phase structure and considered battery degradation in the rerouting of the charging stations. However, they assumed that routes are given as priori, and thus dealt with the assignment of routes to the vehicles at first. Then, they considered the battery degradation cost for determining the charge schedules. Rohrbeck et al. (2018) included the option of replacing the aged battery in their multi-period model for locating the charging stations. Nonetheless, they did not consider the routing decisions. Pelletier et al. (2018) formulated a detailed battery degradation cost structure and integrated it into their mathematical model for the charge scheduling of the electric freight vehicles (EFVs). However, they utilized a set of fixed routes, which are known in advance, as an input parameter. Hence, they did not observe the changes in the routes as a result of battery degradation cost and were only concerned to find the charge schedules of the EFVs. Wang et al. (2020) considered battery degradation in terms of capacity loss while determining the schedules of electric bus fleets. Besides the fact that they utilized a sequential approach, nevertheless, they also do not make any routing decisions. Zang et al. (2022) designed a column generation algorithm to solve the EVRPTW with nonlinear battery degradation costs. However, their algorithm is limited to solving only small-size instances, and they did not propose a solution methodology to solve large-size instances. Furthermore, they took the battery unit price much higher than the one in real life. Moreover, they found solutions without respecting the minimum number of vehicles of the problem instances. Finally, they compared cost savings within the results of their three

proposed mathematical models without considering the distance minimum routes available in the literature. In conclusion, the existing studies remain limited to observing the relationship between changes in the routes and recharging frequencies when battery degradation is considered.

3. BATTERY DEGRADATION

Battery is a power source that transforms stored chemical energy into electrical energy through some chemical reactions. Furthermore, a rechargeable battery is a type of battery that can be reused many times through discharge and recharge cycles. They have a vast area of usage from smartphones to automobiles. In today's world, a huge amount of investment is made to improve battery technology. In this study, we consider EVs equipped with lithium-ion battery packs, which we will refer to as battery throughout the thesis.

Vehicle batteries are consumer goods whose performance decreases as they age like all rechargeable batteries. They provide a limited useful economic life of about 2000 cycles, which is expected to double in the near future (Pelletier et al, 2016). Cycle and calendar aging are two main concepts to explain battery degradation. The former represents the deterioration of the battery during its discharge and recharge cycles, whereas the latter corresponds to the deterioration when the battery is not utilized, i.e. while being stored (Pelletier et al., 2017).

Cycle aging is subject to many factors such as temperature, depth of discharge (DOD) and recharging/discharging rates (Pelletier et al., 2017). DOD refers to the ratio of recharged/discharged amount of energy divided by the battery capacity. On the other hand, calendar aging mainly depends on the temperature of the environment where the battery is stored, time for storage and stored SOC level when the battery is not operated (Barré et al., 2013). SOC corresponds to the amount of charge that the battery currently has divided by its capacity.

Barré et al. (2013) and Pelletier et al. (2017) examined a wide range of studies in which battery degradation is modeled. Among them, we focus on the discrete model devised by

Han et al. (2014), which can be easily implemented within the mathematical formulation of the routing problem. According to this study, battery manufacturers specify the life span of their batteries as the achievable cycle count (ACC) for different DOD values where the battery is discharged from fully charged. ACC-DOD graph illustrated in Figure 3.1 shows that the battery life shortens as the amount of energy discharged increases.

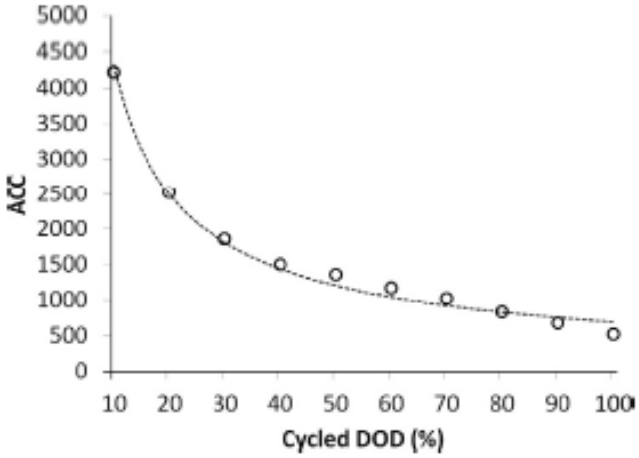

Figure 3.1. ACC-DOD Graph for a Lithium-Ion Battery (Han et al., 2014)

The battery degradation also depends on the initial SOC level in the battery before discharging. Han et al. (2014) distributed the battery price into each unit of energy charged or discharged by considering the initial SOC level of the battery before charging or discharging in their formulation and refer this to as unit wear cost. This formulation can also be extended such that the wear cost function is obtained for a finite number of equal-length SOC intervals as in Equation (3.1). Let $D = \{1, \dots, n_d\}$ denote the set of SOC intervals in which each interval $d \in D$ has a lower and upper SOC bounds of LB^d and UB^d, respectively. Each SOC interval has the same length of $L = LB^d - UB^d$ in percentages. The wear cost $W(LB^d)$ is incurred per kWh charged or discharged within the interval $[LB^d, UB^d]$. The energy amount within each SOC interval in terms of kWh is represented by Δq.

$$Battery\ Price = 2.ACC(DOD) \sum_{\substack{d \in D \\ LB^d \geq 1 - DOD}} W(LB^d)\Delta q \quad DOD \in \{L, 2L, \dots, 1.0\} \quad (3.1)$$

For example, if we utilize 25% DOD intervals, i.e. $L = 0.25$, then we form the set of equations for 4 discrete intervals as shown in Equation set (3.2). In this equation set, Δq

corresponds to an energy amount equal to 25% of the battery capacity. By applying the function illustrated in Figure 3.1, the ACC values are found as 2089, 1204, 872 and 694 for 25%, 50%, 75% and 100% DOD values, respectively. Battery price can be calculated by multiplying the battery capacity with a unit cost of \$150/kWh (see Nykvist et al., 2019). In this way, battery wear cost for each SOC interval, i.e. $W(LB^d)$, can be determined.

$$
\begin{aligned}
W(0.75) &= \frac{Battery\ Price}{ACC(0.25).2.\Delta q} \\
W(0.50) + W(0.75) &= \frac{Battery\ Price}{ACC(0.50).2.\Delta q} \\
W(0.25) + W(0.50) + W(0.75) &= \frac{Battery\ Price}{ACC(0.75).2.\Delta q} \\
W(0.00) + W(0.25) + W(0.50) + W(0.75) &= \frac{Battery\ Price}{ACC(1.00).2.\Delta q}
\end{aligned}
\tag{3.2}
$$

Since the $ACC(DOD)$ function decreases with DOD, the wear cost function is increasing when the open form of Equation (3.1) is considered. This means that operating a battery in higher SOCs is more harmful to its state of health (SOH). For instance, consider two EVs EV1 and EV2 such that their batteries are currently at 40% and 20% SOC levels, respectively. Suppose that a journey that requires 20% DOD must be undertaken by one of them. Both EVs can feasibly complete the journey. Figure 3.2 summarizes the example in which changes in the SOC of the EVs are represented with solid lines whereas dashed lines show the battery wear costs (WC) formed resulting from this trip. If EV1 is used, then its SOC will reduce to 20% at the end of its journey. Otherwise, EV2 is used, and its battery will be empty at the end of its journey. On the other hand, the wear cost $W(.)$ is an increasing function of the initial SOC level. If the unit costs found by Equation set (3.2) are considered, EV2 will incur 8.8% less wear cost than that of EV1 even though the same amount of energy is consumed.

EVs are expected to return to the depot with empty or near-empty batteries with the increasing wear cost structure. Hence, this cost structure also alleviates the effect of calendar aging since storing the battery with higher SOC values is more detrimental to its SOH.

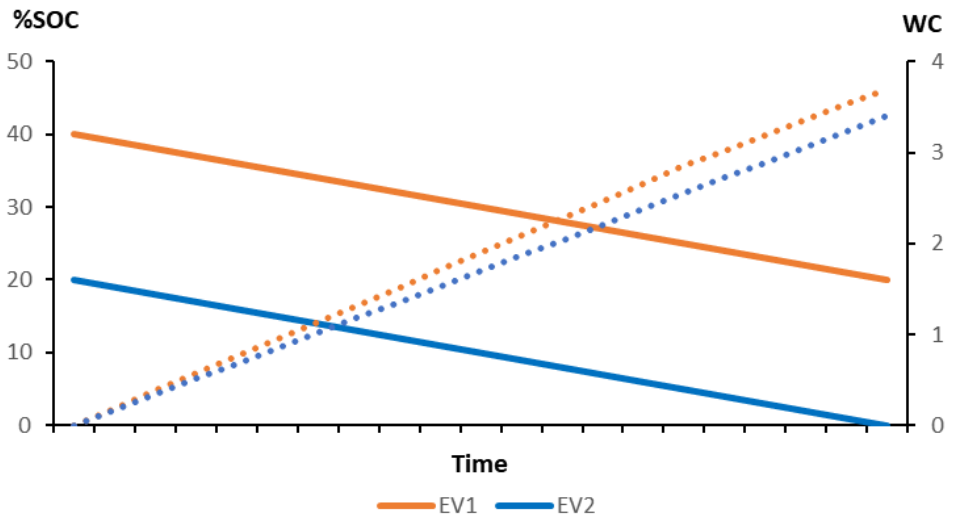

Figure 3.2. Example of change in SOC levels and battery wear costs of two EVs that incurred the same DOD

Note that the battery wear cost function might not always be monotonically increasing, and other general formulations may be used to represent it. However, we assume a monotonically increasing battery wear cost with respect to the initial SOC value to benefit from this characteristic in formulating the mathematical models of the routing problems that we address.

4. THE ELECTRIC TRAVELING SALESMAN PROBLEM WITH TIME WINDOWS BY CONSIDERING BATTERY DEGRADATION

The electric traveling salesman problem (ETSP) is an extension of the TSP where an EV is employed to perform logistics operations instead of an ICEV. Roberti and Wen (2016) introduced the ETSPTW, provided its mathematical model and proposed a VNS algorithm to solve it. In this chapter, we describe the ETSPTW-BD and provide the mathematical model of the problem.

4.1. Problem Description

We address the ETSPTW by following the modeling convention and notation in Schneider et al. (2014) and Roberti and Wen (2016) for ease of understanding. The ETSPTW deals with determining the minimum cost tour of an EV that serves all customers by respecting their time windows. The EV can recharge its battery at any charging station en route and with any amount of energy. A single recharging visit is allowed between two consecutive customers which is a more realistic approach when the industrial practice is considered. Without loss of generality, we assume that the battery of the EV is utilized between its 10% and 90% of its capacity and the recharging time is linearly proportional to the amount of energy transferred. In addition, we take into account the cost associated with the degradation of the battery. Battery degradation is not a static measure and varies according to the SOC and DOD values as explained in Chapter 3. In this chapter, we adopt the modeling approach of Pelletier et al. (2018) who devised constraints and parameters for several distinct wear cost functions to incorporate the effect of battery degradation on the charge schedule of EVs.

Figure 4.1 depicts an example that illustrates how an optimal tour can change when the battery degradation cost is taken into account. The example is based on an instance that we utilized in our experimental study (namely, 'c206c5-s4') and involves five customers and four charging stations. The depot, customers and charging stations are represented with a triangle, circles, and charger icons, respectively. Since the depot is also a charging station, we place a charger icon next to the depot to avoid any confusion. The percentage values along the tour indicate the battery SOC when the EV departs from the depot at the beginning of its trip or from a station after having recharged, and when it arrives at a customer, station, or the depot at the end of its trip. Figure 4.1(a) shows the optimal solution for the distance (energy cost) minimization objective where the customers are visited in the sequence of 1−2−3−4−5 whereas Figure 4.1(b) illustrates the optimal sequence of 1−2−4−3−5 when the objective function minimizes the total cost of energy and battery degradation. We show how the vehicle routes and station visits change in the presence of battery degradation: the EV is recharged three times in Figure 4.1(a) while the number of recharges is four in Figure 4.1(b), and a reduction of 4.6% in the energy plus battery degradation cost is achieved.

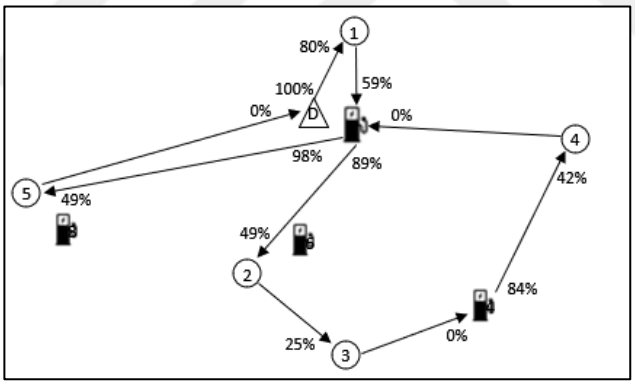

(a) Optimal tour without considering wear cost (Total Cost=1006.4)

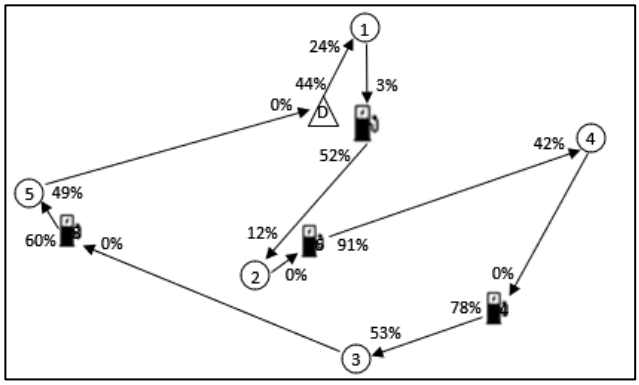

(b) Optimal tour with considering wear cost (Total Cost=960.0)

Figure 4.1. An illustrative example

4.2. Mathematical Model

The notation of the problem is as follows: Let $V = \{1, \dots, n\}$ be the set of customers and F denote the set of charging stations. Nodes 0 and $n+1$ represent the depot where each vehicle departs from node 0 and returns to node $n+1$ at the end of its tour. Then, we define $V_0 = V \cup \{0\}$, $V_{n+1} = V \cup \{n+1\}$ and $V_{0,n+1} = V \cup \{0, n+1\}$. Since the vehicle can visit a charging station more than once, we create an augmented set of stations F' which includes copies of charging stations in F and define $F'_0 = F' \cup \{0\}$, $V' = V \cup F'$, $V'_0 = V' \cup \{0\}$, $V'_{n+1} = V' \cup \{n+1\}$ and $V'_{0,n+1} = V'_0 \cup \{n+1\}$. Now, the problem can be defined on a complete directed graph $G = (V'_{0,n+1}, A)$ in which $A = \{(i,j) | i,j \in V'_{0,n+1}, i \neq j\}$ is the set of arcs.

Each customer $i \in V$ is associated with a service time of s_i and service time window $[e_i, l_i]$. The distance (travel time) from node i to node j is denoted by d_{ij} (t_{ij}). Q is the operational capacity of the battery while g and h represent battery recharge and discharge rates per unit of time, respectively. The maximum tour duration is denoted by l_0. The unit energy cost is denoted by c.

The decision variables τ_i and y_i keep track of the service starting time and battery SOC upon arrival at a node $i \in V'_{0,n+1}$, respectively. The decision variables Y_i denotes the battery SOC on departure from station $i \in F'_0$. If the arc (i,j) traversed, the decision variable x_{ij} takes value 1. To represent the battery degradation in our model, we divided related decision variables and the constraints into two as ones correspond to overnight charging at the depot and ones correspond to recharging at stations. Thus, the decision variables soc_i^d and soc_0^d keep track of how much the portion of SOC interval $d \in D$ is utilized during charging at a station and the depot, respectively. The binary decision variables u_i^d and u_0^d take value of 1 when the SOC interval $d \in D$ is used to charge the vehicle at a charging station and the depot, respectively. Finally, since our wear cost function is non-decreasing, the EV returns to the depot with all its operational battery capacity consumed if it has been recharged at least once en route.

The notation regarding the mathematical model of the ETSPTW-BD is shown in Table 4.1. In what follows, the 0-1 mixed integer linear programming model of the problem is formulated.

Table 4.1. Mathematical notation of ETSPTW-BD

Sets	
V	Set of customers
V_0	Set of customers and departure depot
V_{n+1}	Set of customers and arrival depot
$V_{0,n+1}$	Set of customers, departure and arrival depots
F	Set of charging stations
D	Set of SOC intervals
F'	Set of charging stations with their copies
F'_0	Set of charging stations with their copies and departure depot
V'	Set of customers and charging stations with their copies
V'_0	Set of customers, departure depot and charging stations with their copies
V'_{n+1}	Set of customers, arrival depot and charging stations with their copies
$V'_{0,n+1}$	Set of customers, depots and charging stations with their copies
Parameters	
d_{ij}	Distance between node i and j
t_{ij}	Travel time from node i to node j
s_i	Service time of customer i
$[e_i, l_i]$	Time window of customer i
l_0	Maximum tour duration
Q	Operational battery capacity
g	Recharging rate
h	Total energy consumed to traverse arc (i,j)
c	Unit energy cost
W^d	Wear cost per unit energy charged or discharged within the SOC interval d
L	Length of SOC intervals
UB^d	Upper SOC bound of interval d
LB^d	Lower SOC bound of interval d
Decision variables	
τ_i	Service starting time at customer $i \in V'_{0,n+1}$
y_i	Battery SOC of the EV upon arrival at node $i \in V'_{0,n+1}$
Y_i	Battery SOC of the EV during the departure from node $i \in F'_0$
x_{ij}	1 if the EV traverses arc (i,j); 0 othervise
soc_i^d	Portion of SOC interval $d \in D$ utilized during the recharging at station $i \in F'$
soc_0^d	Portion of SOC interval $d \in D$ utilized during the overnight recharging at the depot
u_i^d	1 if interval $d \in D$ utilized during the recharging at station $i \in F'$; 0 otherwise
u_0^d	1 if interval $d \in D$ utilized during the overnight recharging at the depot; 0 otherwise

$$\text{Min } c\left[\sum_{i\in F'}(Y_i - y_i) + (Y_0 - y_{n+1})\right] + Q\sum_{d\in D}\left[W^d soc_0^d + \sum_{i\in F'} W^d soc_i^d\right] \tag{4.1}$$

subject to

$$\sum_{\substack{j\in V'_{n+1}\\ i\neq j}} x_{ij} = 1 \qquad \forall i \in V_0 \qquad (4.2)$$

$$\sum_{\substack{j\in V_{n+1}\\ i\neq j}} x_{ij} \leq 1 \qquad \forall i \in F' \qquad (4.3)$$

$$\sum_{\substack{i\in V'_0\\ i\neq j}} x_{ij} - \sum_{\substack{i\in V'_{n+1}\\ i\neq j}} x_{ji} = 0 \qquad \forall j \in V' \qquad (4.4)$$

$$\tau_i + \left(t_{ij} + s_i\right)x_{ij} - l_0\left(1 - x_{ij}\right) \leq \tau_j \qquad \forall i \in V_0, \forall j \in V'_{n+1}, i \neq j \qquad (4.5)$$

$$\tau_i + t_{ij}x_{ij} + g(Y_i - y_i) - (l_0 + g.Q)\left(1 - x_{ij}\right) \leq \tau_j \qquad \forall i \in F', \forall j \in V_{n+1}, i \neq j \qquad (4.6)$$

$$e_j \leq \tau_j \leq l_j \qquad \forall j \in V'_{0,n+1} \qquad (4.7)$$

$$0 \leq y_j \leq y_i - \left(h \cdot d_{ij}\right)x_{ij} + Q\left(1 - x_{ij}\right) \qquad \forall i \in V, \forall j \in V'_{n+1}, i \neq j \qquad (4.8)$$

$$0 \leq y_j \leq Y_i - (h \cdot d_{ij})x_{ij} + Q\left(1 - x_{ij}\right) \qquad \forall i \in F'_0, \forall j \in V_{n+1}, i \neq j \qquad (4.9)$$

$$y_i \leq Y_i \leq Q \qquad \forall i \in F'_0 \qquad (4.10)$$

$$Q\sum_{d\in D} soc_i^d = Y_i - y_i \qquad \forall i \in F' \qquad (4.11)$$

$$Q\sum_{d\in D} soc_0^d = Y_0 - y_{n+1} \qquad (4.12)$$

$$0 \leq soc_i^d \leq L.u_i^d \qquad \forall i \in F', \forall d \in D \qquad (4.13)$$

$$0 \leq soc_0^d \leq L.u_0^d \qquad \forall d \in D \qquad (4.14)$$

$$Q.soc_i^d \leq Q.UB^d - y_i + Q(1 - u_i^d) \qquad \forall i \in F', \forall d \in D \qquad (4.15)$$

$$Q.soc_0^d \leq Q.UB^d - y_{n+1} + Q(1 - u_0^d) \qquad \forall d \in D \qquad (4.16)$$

$$x_{ij} \in \{0,1\} \qquad \forall i \in V'_0, \forall j \in V'_{n+1}, i \neq j \qquad (4.17)$$

$$u_i^d \in \{0,1\} \qquad \forall i \in F', \forall d \in D \qquad (4.18)$$

$$u_0^d \in \{0,1\} \qquad \forall d \in D \qquad (4.19)$$

The objective function (4.1) minimizes the total cost of energy consumption and battery degradation. The first two terms of the objective function correspond to total energy consumption from recharging at the stations and the depot, respectively. The battery degradation cost resulting from charging activities at the depot and stations are represented with the following two terms. Constraints (4.2) guarantee that the tour starts from the depot and each customer is visited exactly once. Constraints (4.3) ensure that each station can be visited at most once. The flow conservation constraints are represented by constraints (4.4). Constraints (4.5) and (4.6) set service start times at customers and stations, respectively, and constraints (4.7) respect the service time windows of the customers. Constraints (4.8) and (4.9) keep track of the battery SOC upon arrival at a customer and departure from a station/depot, respectively, whereas constraints (4.10) set the bounds for the SOC. Constraints (4.11) and (4.12) distribute the total amount of energy recharged at the stations and the depot overnight to related SOC intervals, respectively. Constraints (4.13) and (4.14) set bounds to the utilization of SOC intervals for the recharging at the stations and the depot, respectively. Constraints (4.15) and (4.16) make sure that the SOC interval takes a positive value if the battery SOC upon arrival at the station/depot is less than the upper bound of the corresponding SOC interval. Since we employ a non-decreasing wear cost function, the model will use lower SOC intervals due to the minimization objective function. Finally, constraints (4.17)–(4.19) define the binary decision variables. Note that regardless of the common assumption in the literature, we did not set the EV's initial battery level during departure from the depot to full capacity since the high level of battery SOCs result in more battery degradation when a non-decreasing wear cost function is considered.

5. SOLUTION METHODOLOGY

We develop an algorithm, MatHeur, which is a VNS-based matheuristic enhanced with a post-optimization method to solve the ETSPTW-BD.

VNS is a metaheuristic method utilized to solve combinatorial optimization problems. The method was developed by Mladenović and Hansen (1997), and it basically consists of two phases which are the local search and perturbation (shaking). The local optimum solutions are obtained with the application of local search while the same local optimum solution is avoided by implementing the shaking where neighborhood sizes are systematically enlarged in both phases (Hansen et al., 2010). Since then, various forms of VNS algorithms have been employed to solve different TSP variants such as TSPTW (da Silva and Urrutia, 2010; Mladenović et al., 2012), ETSPTW (Roberti and Wen, 2016) and HEVTSPTW (Doppstadt et al., 2020). The method has also been successfully implemented to solve the VRP and its extensions, e.g. EVRPTW (Schneider et al., 2014), VRP with intermediate stops (Schneider et al., 2015), electric LRP (Hof et al., 2017; Almouhanna et al. 2020), multi-depot GVRP (Sadati and Çatay, 2021) and EVRP (Zhu et al., 2020), EVRPTW with time-dependent energy prices (Lin et al., 2021), time-dependent EVRPTW (Lu et al., 2020; Wang et al., 2020) and EVRP with flexible deliveries (Sadati et al., 2022).

The MatHeur starts with the construction of a TSP tour with a pseudo-random insertion algorithm. Then, this solution $\boldsymbol{x}$ is set to the best TSPTW tour $\boldsymbol{x}^*$ and shaking is applied to $\boldsymbol{x}^*$. Next, the cyclic local search is implemented. If the solution obtained after the local search phase produces less cost than $\boldsymbol{x}^*$, then $\boldsymbol{x}$ is assigned to $\boldsymbol{x}^*$, and the counters for shaking operators k and non-improving iterations $nonImpIterCount$ are reset to 1 and 0, respectively. Also, an ETSPTW-BD solution $\boldsymbol{y}$ is obtained from the local optimum $\boldsymbol{x}^*$

by solving the mathematical model of the fixed-tour vehicle-charging problem (FTVCP) by considering battery degradation; and if the solution $\boldsymbol{y}$ is feasible and has a better objective function value than the previous ones, $\boldsymbol{y}$ is set to $\boldsymbol{y}^*$. Otherwise, i.e. if $\boldsymbol{x}^*$ is not improved, k and $nonImpIterCount$ are increased by one, and the shaking is performed on the solution $\boldsymbol{x}^*$ with a larger neighborhood except the case when k reaches its maximum and reset to 1. This procedure is repeated until the limits for the number of iterations ($\#Iter$) and of non-improving iterations ($\#NonImpIter$) are exceeded. We propose a mechanism called *Slack* which ensures sufficient time for recharges after customer visits in the construction and local search phases. We also utilize a parameter named *CL Size* to restrict the search space during the phases of construction and local search. The definitions of *Slack* and *CL Size* are provided in the following section. We elaborate the phases of the MatHeur in the following subsections. The pseudocode of the algorithm is provided in Algorithm 5.1

Algorithm 5.1: MatHeur

$\boldsymbol{y}^* \leftarrow null$ // Best ETSPTW-BD solution
$\boldsymbol{y} \leftarrow null$ // Cuurent ETSPTW-BD solution
$iterCount \leftarrow 0$, $nonImpIterCount \leftarrow 0$
Set of shaking neighborhood structures S_k $\{k = 1, \dots, k_{max}\}$
$k \leftarrow 1$
1 $\boldsymbol{x} \leftarrow$ Construct the initial tour
2 $\boldsymbol{x}^* \leftarrow \boldsymbol{x}$ // Best TSPTW solution
3 **while** $(iterCount < \#Iter) \& (nonImpIterCount < \#NonImpIter)$
4 Select a random solution $\boldsymbol{x}$ from the k^{th} neighborhood $S_k(\boldsymbol{x}^*)$ of $\boldsymbol{x}^*$ // Shaking
5 $\boldsymbol{iterCount++}$
6 $Local\ Search(\boldsymbol{x}, \boldsymbol{x}^*)$
7 **if** $(cost(\boldsymbol{x}) < cost(\boldsymbol{x}^*))$
8 $\boldsymbol{x}^* \leftarrow \boldsymbol{x}$
9 $k \leftarrow 1$
10 $nonImpIterCount \leftarrow 0$
11 $\boldsymbol{y} \leftarrow FTVCP(\boldsymbol{x}^*)$ // Create an ETSPTW-BD solution
12 **else if** $(k = k_{max})$
13 $k \leftarrow 1$
14 $nonImpIterCount++$
15 **else**
16 $k++$
17 $nonImpIterCount++$
18 **end if**
19 **if** $(cost(\boldsymbol{y}) < cost(\boldsymbol{y}^*))$
20 $\boldsymbol{y}^* \leftarrow \boldsymbol{y}$
21 **end if**
22 **end while**
23 **return** $\boldsymbol{y}^*$

5.1. Initial Tour Construction

The initial tour is obtained using an insertion heuristic. First, the farthest customer from the depot is inserted into the tour. Then, unassigned customers are sorted in a list in ascending order of their late arrival times. One of the first four customers in the list is randomly selected. Next, the cheapest insertion is performed by calculating the insertion costs of the selected customer to all possible positions in the tour. If an insertion results in time-window violations for the inserted and its successor nodes, a penalty cost is added to the insertion cost by multiplying a sufficiently large number with the sum of each violated time unit. This procedure is repeated until no customer remains unassigned, and a customer sequence is obtained.

Since the EVs have limited driving ranges, recharges take place along the tour. However, recharges take a significant amount of time when compared to the refueling time of ICEVs. Hence, we design a new mechanism to be used in the construction and local search phases of MatHeur and refer it to as S*lack*. We propose reserving a certain amount of time with respect to the maximum tour duration for each customer during determining the sequence by considering possible recharges after customer visits. Thus, a customer is visited before its late arrival time by also respecting this period. For example, let the EV must serve all the customers between 08:00-18:00 which makes the horizon of the day 10 hours. If a customer must be served before 12:00 and *Slack* is 1%, 0.1 hours, i.e. 6 minutes, is reduced from the customer's service time window. In this way, we ensure the customer is visited before 11:54 by considering potential recharging visits that might take place after this trip. Thus, we attempt to provide a sufficient amount of time for recharging between consecutive customer visits and to arrive at the next customers on time by departing from the customers a little bit earlier than required. We show the benefit of the proposed mechanism in Section 6.2.

We also adapt a parameter, called candidate list size (*CL Size*), to MatHeur which limits the number of candidate positions that a customer can be located in the tour during the construction and local search phases. A position for a customer node is only evaluated if its total distance to the predecessor and successor nodes in the new position is below some certain threshold. Basically, the solution space becomes narrower, and the computational effort is only made in the promising regions in the neighborhood. For instance, let this parameter be 50, then the evaluation is made only if the insertion cost of a customer is

below the insertion cost of the 50th best customer for that position. If this parameter is 1, then only the best insertion can be applied, and no restrictions are available with the parameter value of n which is the number of customers in the problem instance. We also demonstrate the impact of this parameter in Section 6.2.

5.2. Shaking

A random tour is obtained using shaking operators during the shaking phase of the MatHeur. The only shaking neighborhood operator in the MatHeur is λ-Move which moves randomly selected λ customers to random positions in the tour without seeking time windows feasibility. We also considered λ-Exchange, which swaps the position of randomly selected λ customer pairs, as a shaking neighborhood. However, our preliminary results showed that λ-Exchange increases the runtime of the algorithm significantly without providing much benefit in the solution quality.

Algorithm 5.2: $Local\ Search(\boldsymbol{x}, \boldsymbol{x}^*)$

Set of LS neighborhood structures I_m $(m = 1, \dots, m_{max})$
$m \leftarrow 1$
1 $\boldsymbol{x}' \leftarrow \boldsymbol{x}$ // Incumbent solution
2 **while** $(m \leq m_{max})$
3 Apply I_m on $\boldsymbol{x}$
4 **if** $(cost(\boldsymbol{x}) < cost(\boldsymbol{x}^*))$
5 **break**
6 **else if** $(cost(\boldsymbol{x}) < cost(\boldsymbol{x}'))$
7 $\boldsymbol{x}' \leftarrow \boldsymbol{x}$
8 $m \leftarrow 1$
9 **else**
10 $m++$
11 **end if**
12 **end while**

5.3. Local Search

The random solution obtained after the shaking phase is improved by applying local search (LS). The LS phase of MatHeur has the following neighborhood structures: *Move*, *Exchange* and 2-*Opt*. A customer is selected and located to a new position in the tour with the *Move* operator. The positions of two customers are replaced in the *Exchange* operator. 2- *Opt* selects two arcs in the tour and reverses the order of customers that are positioned between these two arcs. We apply the LS in a cyclic manner, i.e. the algorithm returns to the first LS operator (*Move*), if the solution improves with one of the LS operators. The

first-improvement scheme is employed in all operators. Note that evaluations during the LS are only made for the options that satisfy the time window compatibility of the customer nodes. As in the construction phase, the penalty cost for time windows violations is also considered during the evaluations. The LS is expected to generate good feasible solutions for inserting the charge stations without requiring any repair mechanism since we incur high penalty costs and implement *Slack*. The pseudocode of the LS is given in Algorithm 5.2.

5.4. Fixed-Tour Vehicle-Charging Problem (FTVCP)

We make recharging-related decisions in the tour by employing a post-optimization technique. The model described in Section 4.2 can be utilized by fixing the x_{ij} variables according to the fixed sequence of customers obtained after the LS phase. However, this approach is computationally burdensome, and a more efficient method, the fixed-route vehicle-charging problem (FRVCP), was presented in the literature. This problem is introduced by Montoya et al. (2017) based on Suzuki (2014), and basically decides the stations to be visited and energy amounts at customer and station nodes on a fixed sequence of customers. Hence, we extend the mathematical model of the FRVCP by considering battery degradation and solve it on CPLEX for each local optimum solution generated by the LS phase of MatHeur. Since our problem is an extension of the TSP, we refer to this problem as the fixed-tour vehicle-charging problem (FTVCP).

We followed the notation used in Keskin and Çatay (2018) originated from Bruglieri et al. (2016), and the formulation has some certain notation differences with respect to the model presented in Section 4.2. Let $\bar{V} = \{ c_1, c_2, \dots, c_n\}$ be the ordered set of customers visited by the EV where c_i corresponds to the customer in the i^{th} position of the fixed tour. We define $\bar{V}_0 = \{0\} \cup \bar{V}$ and $\bar{V}_{n+1} = \bar{V} \cup \{\mathrm{n}+1\}$ so that the sequence has the departure and arrival depots, respectively. If station $j \in F$ is visited after the departure from customer c_i on the tour, x_{ij} takes the value of 1. The decision variable $\theta_{i,i+1}$ keeps track of the amount of energy transferred if a recharging visit occurs between customers c_i and c_{i+1} on the tour. The binary decision variable $u^d_{i,i+1}$ takes the value of 1 if the EV is recharged during its trip from customer c_i to customer c_{i+1}, and the decision variables $\theta_{i,i+1}$ and $soc^d_{i,i+1}$ keep track of the amount of energy transferred and how much portion of SOC interval $d \in D$ is utilized during this recharging visit, respectively.

$$Min \sum_{i \in \bar{V}_0} c.\theta_{i,i+1} + c(y_0 - y_{n+1}) + Q \sum_{d \in D} \left[W^d soc_0^d + \sum_{i \in \bar{V}_0} W^d soc_{i,i+1}^d \right] \quad (5.1)$$

subject to

$$\sum_{j \in F} x_{ij} \leq 1 \qquad \forall i \in \bar{V}_0 \quad (5.2)$$

$$\tau_i + s_i + t_{i,i+1} \left(1 - \sum_{j \in F} x_{ij} \right) + \sum_{j \in F} (t_{ij} + t_{j,i+1}) x_{ij} + g.\theta_{i,i+1} \leq \tau_{i+1} \qquad \forall i \in \bar{V}_0 \quad (5.3)$$

$$e_i \leq \tau_i \leq l_i \qquad \forall i \in \bar{V}_{n+1} \quad (5.4)$$

$$y_i - h \left[d_{i,i+1} \left(1 - \sum_{j \in F} x_{ij} \right) + \sum_{j \in F} (d_{ij} + d_{j,i+1}) x_{ij} \right] + \theta_{i,i+1} = y_{i+1} \qquad \forall i \in \bar{V}_0 \quad (5.5)$$

$$y_i - h \sum_{j \in F} d_{ij} x_{ij} \geq 0 \qquad \forall i \in \bar{V}_0 \quad (5.6)$$

$$\theta_{i,i+1} \leq Q \sum_{j \in F} x_{ij} \qquad \forall i \in \bar{V}_0 \quad (5.7)$$

$$\theta_{i,i+1} \leq Q - (y_i - h \sum_{j \in F} d_{ij} x_{ij}) \qquad \forall i \in \bar{V}_0 \quad (5.8)$$

$$Q \sum_{d \in D} soc_{i,i+1}^d = \theta_{i,i+1} \qquad \forall i \in \bar{V}_0 \quad (5.9)$$

$$Q \sum_{d \in D} soc_0^d = y_0 - y_{n+1} \quad (5.10)$$

$$0 \leq soc_{i,i+1}^d \leq L.u_{i,i+1}^d \qquad \forall i \in \bar{V}_0, \forall d \in D \quad (5.11)$$

$$0 \leq soc_0^d \leq L.u_0^d \qquad \forall d \in D \quad (5.12)$$

$$Q.soc_{i,i+1}^{d} \leq Q.UB^{d} - \left(y_i - h \sum_{j \in F} d_{ij} x_{ij} \right) + Q(1 - u_{i,i+1}^{d}) \qquad \forall i \in \bar{V}_0, \forall d \in D \qquad (5.13)$$

$$Q.soc_{0}^{d} \leq Q.UB^{d} - y_{n+1} + Q(1 - u_{0}^{d}) \qquad \forall d \in D \qquad (5.14)$$

$$x_{ij} \in \{0,1\} \qquad \forall i \in \bar{V}_0, \forall j \in F \qquad (5.15)$$

$$u_{i,i+1}^{d} \in \{0,1\} \qquad \forall i \in \bar{V}_0, \forall d \in D \qquad (5.16)$$

$$u_{0}^{d} \in \{0,1\} \qquad \forall d \in D \qquad (5.17)$$

The objective function (5.1) minimizes the total cost of the tour where the first two terms represent the energy cost and the last two corresponds to the battery degradation cost. Constraints (5.2) guarantee that at most one recharging visit occurs between two consecutive customers. Time windows feasibility of customer and depot nodes are satisfied with constraints (5.3) and (5.4). Constraints (5.5) keep track of the battery SOC upon arrival at the customer and depot nodes. If a recharging visit takes place between two consecutive customers, constraints (5.6) ensure that the SOC when the EV departs from the preceding customer is sufficient to reach the charging station. If a charging station is visited between customers c_i and c_{i+1}, then constraints (5.7) guarantee that the amount of energy transferred is positive and constraints (5.8) limit the amount with an upper bound. The total amount of energy transferred at charging stations and at the depot overnight are distributed to the SOC intervals by constraints (5.9) and (5.10), respectively. Constraints (5.11) and (5.12) set upper and lower bounds on SOC intervals for recharges at the station and depot, respectively. Constraints (5.13) and (5.14) ensure that the SOC intervals take positive values only when the battery SOC of the EV upon its arrival at the charging stations or depot is less than the upper bound of the related SOC interval. Binary decision variables are defined by constraints (5.15)-(5.17).

We also apply the pre-processing procedures proposed by Keskin and Çatay (2018) and reduce the size of set F without dangering not achieving the optimal solution. Hence, the number of decision variables decreases, and the computational time required to solve the problem shortens significantly.

6. EXPERIMENTAL STUDY

This section first introduces the experimental setting. Then, we present the parameter tuning of MatHeur and validate its performance. Next, the effect of battery degradation on route and charge plans is demonstrated with computational studies. Finally, we provide sensitivity analyses regarding the problem parameters and a trade-off analysis with a multi-start version of MatHeur. We performed our experimental study on a Windows 10 OS computer equipped with an Intel i7-8700 3.20 GHz CPU and 32 GB RAM. MatHeur and the models presented in Sections 4.2 and 5.4 were coded in Java, and the models were solved using CPLEX 12.9.0 in the default mode.

6.1. Experimental Setting

To investigate the impact of the battery wear cost on the route and charging schedules, we conduct experimental tests using small- and large-size instances. Our small-size data includes a subset of small-size EVRPTW instances that were generated by Schneider et al. (2014) where a single EV is employed in the optimal or best-known distance minimum solutions in 13 instances. The details about this dataset are presented in the Section 7.2.1. We also benefit from the small-size ETSPTW instances that were generated by Roberti and Wen (2016) based on the TSPTW instances of Gendreau et al. (1998). These instances consist of 20 customers, and the time window widths are 120-, 140-, 160-, 180- and 200-time units. There are 5 instances associated with each time-window width and two versions of each instance exist involving 5 and 10 charging stations. Hence, the dataset includes 5×5×2=50 small-size instances in total.

Our large-size instances are based on the large-size ETSPTW instances that were generated by Roberti and Wen (2016) using the TSPTW instances of Ohlmann and

Thomas (2007). This dataset is mainly classified into two groups each involving 5 and 10 charging stations. Then, each subgroup involves 15 instances involving 150-customers and 10 instances involving 200-customers. Hence, the dataset includes 2×(15+10)=50 large-size instances in total. Time window widths in these instances vary from 120 to 160-time units in 150-customer instances and from 120 to 140-time units in 200-customer instances. In the nomenclature of the instances generated by Roberti and Wen (2016), the numbers beside 'n', 'w' and 's' represent the number of customers, time windows width and the number of charging stations, respectively, while the number after the dot shows the version of the data.

The unit penalty cost applied for time windows violations found during the construction and local search phases is set to 100. We set $n_d = 4$ and $L = 1/4 = 0.25$ following the base case scenario of Pelletier et al. (2018). Hence, the upper and lower bounds of SOC intervals are $LB^d = \{0, 0.25, 0.5, 0.75\}$ and $UB^d = \{0.25, 0.5, 0.75, 1\}$. They considered battery unit cost as \$410/kWh and calculated battery wear cost for these four intervals as 0.48, 0.52, 0.58 and \$0.79/kWh, respectively. As we explained in Chapter 3, battery unit cost can be assumed as \$150/kWh and so wear costs for these four intervals become 0.17, 0.19, 0.21 and \$0.29/kWh, respectively. What is more, both Schneider et al. (2014) and Roberti and Wen (2016) assumed that the EV travels one unit of distance in one unit of time by consuming one unit of energy. So, we set the unit energy cost $c = 1$ to be able to compare our results with those reported in the literature. However, the average industrial electricity price was \$0.0681/kWh in 2019 in the U.S (EIA, 2020). Thus, we adapted the wear costs calculated above to our problem by keeping the ratio between the unit energy cost parameter and the unit electricity price. So, our $W^d = \{2.56, 2.78, 3.10, 4.22\}$.

The distances provided in the Roberti and Wen (2016) dataset are rounded to integer values and do not satisfy the triangle property. In the original TSPTW data, the Euclidean distances were first rounded down to the nearest integer values. Then, some adjustments were made so that triangle inequality holds. However, this approach reduces distance measures once more time, does not guarantee the triangle inequality and results in overestimating the results. Fleming et al. (2013) demonstrated the negative effects of triangular inequality violations on the VRP. Furthermore, Roberti and Wen (2016) located four and nine charging stations in addition to the depot for each TSPTW instance. They calculated the distances between the customers and charging stations as the Euclidean

distance and rounded them to the nearest integer. Hence, the distance measures between customers and the distance measures between a customer and a charging station were not given in a consistent manner, and the triangle inequality still does not hold in their data. In addition, different tours might yield the same optimal or best-known objective function value (OFV) in the problem since the distance matrix consists of integer values. Hence, differentiating the optimal or best-known tour might not be possible since multiple solutions can have the same OFV, and this impairs our solution approach that employs good TSPTW tours to obtain solutions that take into account the wear cost. We provide examples of different ETSPTW tours having the same OFV in Table 6.1. The nomenclature of the problem instances is depicted under column 'Instance'. 'TD' indicates the total distance covered in the optimal tours. The sequence of nodes visited is reported under column 'Tour'. Node 0 is the depot and the charging station, nodes 1-20 are customers and nodes 21-24 are the charging stations. We also observed that the number of different tours that yield the same OFV increases as the problem size grows. As a result, we decided to calculate the distances by using the Euclidean distance formula in two decimal places. Since we eliminate the overestimation, the total distance of the TSPTW tours is significantly increased. To be able to cover increased distances, we extend the length of planning horizon and late arrival time values of each customer node in the datasets by a certain rate. Since our algorithm finds the best-known solutions (BKSs) in the TSPTW setting, which we will demonstrate it in the following section, we find the rates for increasing the late arrival times by proportioning the BKSs obtained with the integer and two-decimal distance measures. We provide the rates in Appendix A. Finally, we utilized the same coordinates for charging station locations and the same parameter values of g, h and Q as presented in Roberti and Wen (2016) without altering them. We only assume as Q is the operational battery capacity.

Table 6.1. Examples of tours having the same total distance

Instance	TD	Tour
n20w120s5.1	271	0,6,16,9,19,17,18,12,10,11,5,1,15,2,21,7,4,13,20,24,3,8,14,21,0
		0,6,16,9,19,17,22,18,12,10,11,5,1,15,2,21,7,4,13,20,24,3,8,14,21,0
n20w120s5.2	225	0,1,14,18,4,8,21,19,16,11,15,23,5,7,3,20,17,12,9,10,23,6,2,13,0
		0,1,14,18,4,8,21,19,16,11,15,23,5,7,3,20,17,12,10,9,23,6,2,13,0
n20w120s5.5	249	0,19,13,11,7,16,18,3,8,21,17,2,5,14,10,4,24,6,9,15,12,22,1,20,0
		0,19,13,11,7,16,18,3,8,21,17,2,5,14,10,4,24,9,6,15,12,22,1,20,0
		0,19,13,11,7,16,18,3,8,21,17,2,5,10,14,4,24,9,6,15,12,22,1,20,0
		0,19,13,11,7,16,18,3,8,21,17,2,5,10,14,4,24,6,9,15,12,22,1,20,0

6.2. Parameter Tuning

The MatHeur utilizes 5 parameters which are shaking level (λ), *Slack*, *#NonImpIter*, *#Iter* and *CL Size*. To tune these parameters, we selected a subset consisting of five 150- and five 200-customers instances as follows: n150w120s5.2, n150w140s5.1, n150w140s5.4, n150w160s5.2, n150w160s5.3, n200w120s5.1, n200w120s5.4, n200w120s5.5, n200w140s5.3 and n200w140s5.4. The parameters are sequentially tuned from λ to *CL Size*. We set the initial values of λ, *Slack*, *#NonImpIter*, *#Iter* and *CL Size* to 6, 0%, $3n$, $3n$ and n, respectively. To tune each parameter, we performed 25 runs per problem instance and calculated the average percentage deviation from the average of the best solutions obtained (Δ%). The value with the smallest Δ% was selected. This procedure was repeated until all parameters had been tuned. If more than one value provides the same Δ%, we favored the smaller value. The values tested and their corresponding Δ% are presented in Table 6.2. The selected values are shown in bold.

Table 6.2. Parameter tuning

Parameter	Values (Δ%)					
λ	6	8	10	12	**14**	16
	(0.10)	(0.29)	(0.13)	(0.44)	**(0.00)**	(0.16)
Slack	0%	0.5%	**1%**	1.5%	2%	-
	(1.05)	(0.48)	**(0.00)**	(0.33)	(0.50)	
#NonImpIter	0.25*n*	0.375*n*	**0.5*n***	0.75*n*	*n*	-
	(0.51)	(0.13)	**(0.00)**	(0.00)	(0.00)	
#Iter	*n*	*2n*	3*n*	**4*n***	5*n*	-
	(0.43)	(0.36)	(0.13)	**(0.00)**	(0.00)	
CL Size	0.05*n*	0.1*n*	**0.15*n***	0.25*n*	0.5*n*	*n*
	(0.16)	(0.08)	**(0.00)**	(0.08)	(0.18)	(0.37)

6.3. Performance Validation

We validate the performance of MatHeur in several problem settings. We performed 25 runs for each problem instance, and the best solution found by MatHeur is considered in the comparisons.

6.3.1. Validation on the TSPTW

We test the performance of MatHeur on the large-size TSPTW problem instances of Ohlmann and Thomas (2007). Since the problem does not include EVs, we set S*lack* to

0% and did not solve the FTVCP throughout the execution of MatHeur. Our algorithm finds the BKSs in all instances, which are reported in Da Silva and Urrutia (2010), even if the distance measures are integer as explained in Section 6.1.

6.3.2. Validation on the ETSPTW

We also demonstrate the effectiveness of MatHeur in the ETSPTW setting. We compare the solution quality and the run time of Matheur with CPLEX in small-size problem instances with 20 customers. The model presented in Section 4.2 is modified by including the distance minimization objective and not considering battery degradation constraints and solved with CPLEX. We did not restrict the algorithm and set *#NonImpIter* and *CL Size* to 4*n* and *n*, respectively since the problem sizes are small. Furthermore, each local optimum solution obtained after any LS operator is sent to the FTVCP in which the objective is distance minimization. The results are shown in Table 6.3. The runtimes required are in seconds and show the average execution time of 25 runs in the case of MatHeur which is reported under 'MatHeur'. Both CPLEX and MatHeur find the optimal solutions. We obtained the same solution quality with less average computational time.

6.3.3. Validation on the ETSPTW-BD

The performance of MatHeur is validated in the original problem, i.e., ETSPTW-BD, as well. The solutions achieved by CPLEX and MatHeur are compared in problem instances with 20 customers. The model presented in Section 4.2 is solved with CPLEX. The parameters of *#NonImpIter* and *CL Size* are set to their upper bounds during the execution of MatHeur since the problem sizes are small. Furthermore, the FTVCP is solved for the local optimal solutions obtained after each LS operator. Table 6.4 presents the results. Column 'CPLEX' reports the OFVs of the solutions obtained with CPLEX. Note that CPLEX was able to provide an upper bound in only 13 out of 50 instances at the end of the 2-hour time limit. So, we only report the solutions for these instances. The best solution found by MatHeur and its average runtime in seconds are presented in the columns 'MatHeur' and 't (s)', respectively. The last column shows the percentage difference between the costs found with CPLEX and MatHeur where a positive value indicates improvement. MatHeur finds better results in all instances within remarkably shorter computation times.

Table 6.3. Comparison of ETSPTW results for 20-customer problems

		Runtime				Runtime	
Instance	TD	CPLEX	MatHeur	Instance	TD	CPLEX	MatHeur
n20w120s5.1	274.48	3.6	0.5	n20w120s10.1	273.37	2.6	0.7
n20w120s5.2*	228.02	386.2	0.6	n20w120s10.2	223.84	302.7	0.6
n20w120s5.3*	297.10	6.5	0.3	n20w120s10.3*	295.47	9.1	0.2
n20w120s5.4	307.17	91.5	0.2	n20w120s10.4	299.80	17.4	0.5
n20w120s5.5	254.63	2.3	0.3	n20w120s10.5	248.52	2.0	0.3
n20w140s5.1	188.20	17.7	0.2	n20w140s10.1	185.56	9.0	0.2
n20w140s5.2	274.47	153.9	0.3	n20w140s10.2	258.74	104.1	0.3
n20w140s5.3	244.16	30.7	0.1	n20w140s10.3	244.13	23.3	0.2
n20w140s5.4*	254.85	536.4	0.6	n20w140s10.4*	244.28	39.7	0.5
n20w140s5.5*	223.60	2.5	0.3	n20w140s10.5*	221.04	4.1	0.3
n20w160s5.1	245.12	9.7	0.3	n20w160s10.1	245.12	19.7	0.4
n20w160s5.2	224.22	17.7	0.4	n20w160s10.2	214.56	13.2	0.6
n20w160s5.3	213.11	1.3	0.3	n20w160s10.3	213.11	2.3	0.3
n20w160s5.4	213.43	30.2	0.3	n20w160s10.4	213.43	45.0	0.3
n20w160s5.5*	251.41	41.0	0.6	n20w160s10.5*	243.11	27.1	0.5
n20w180s5.1	266.88	63.1	0.2	n20w180s10.1	260.07	35.1	0.2
n20w180s5.2	281.35	106.2	0.4	n20w180s10.2	279.89	72.2	0.4
n20w180s5.3	275.27	33.9	0.3	n20w180s10.3	274.95	106.7	0.3
n20w180s5.4	208.51	41.8	0.3	n20w180s10.4	205.50	97.8	0.3
n20w180s5.5	205.78	930.4	0.4	n20w180s10.5	203.74	1568.4	0.4
n20w200s5.1	238.35	469.8	0.2	n20w200s10.1	238.35	67.9	0.2
n20w200s5.2	220.52	69.1	0.3	n20w200s10.2	216.41	37.7	0.3
n20w200s5.3	250.73	73.0	0.3	n20w200s10.3	250.27	93.5	0.3
n20w200s5.4	299.22	413.1	0.4	n20w200s10.4	298.11	398.8	0.5
n20w200s5.5	243.68	60.1	0.5	n20w200s10.5	236.60	90.2	0.5
Average	247.37	143.67	0.35		243.52	127.58	0.38

* Achieved by MatHeur during the parameter tuning with Slack = 0

We also test MatHeur in smaller instances to validate its actual performance in the ETSPTW-BD setting. The dataset of Schneider et al. (2014) is classified into three groups, each involving 5, 10 and 15 customers, and includes 3×12=36 instances in total. Among these instances, we selected 13 instances in which a single EV is employed in the optimal EVRPTW solutions reported in the literature. The settings of CPLEX and MatHeur are the same as in solving the 20-customer instances. We present the results in Table 6.5. The values following ‘c’ and ‘s’ along the instances indicate the number of customers and charging stations in the corresponding instance, respectively. The computational time required by CPLEX and the average runtime of MatHeur are presented in seconds under columns ‘t (s)’, respectively. The optimality of the solutions which are obtained using the

entire runtime of 7200 seconds by CPLEX are not guaranteed. MatHeur finds the same solutions obtained by CPLEX in all 5- and 10-customer instances and achieves better results in 15-customer instances which are indicated in bold. MatHeur requires less computational time on average to obtain better solution quality. Consequently, we believe that the performance of MatHeur is validated with these results.

Table 6.4. Comparison of ETSPTW-BD results for 20-customer problems

Instance	CPLEX	MatHeur	t (s)	%Imp
n20w120s5.1	1034.75	1021.63	0.81	1.27
n20w120s5.2	953.90	875.39	0.53	8.23
n20w120s5.5	1395.54	975.21	0.45	30.12
n20w140s5.2	1206.84	1067.26	0.43	11.57
n20w140s5.3	987.54	909.55	0.15	7.90
n20w140s5.4	1254.21	1024.95	0.29	18.28
n20w160s5.3	1087.94	838.45	0.34	22.93
n20w160s5.4	894.95	798.92	0.52	10.73
n20w160s5.5	1127.29	991.81	0.74	12.02
n20w120s10.1	1058.80	1006.83	0.84	4.91
n20w120s10.5	964.52	938.98	0.55	2.65
n20w140s10.1	892.11	697.28	0.42	21.84
n20w140s10.3	1034.07	895.38	0.16	13.41
Average	1068.65	926.28	0.48	12.76

Table 6.5. Comparison of ETSPTW-BD results for small-size single-EV problems of Schneider et al. (2014)

	CPLEX		MatHeur	
Instance	Cost	t (s)	Cost	t (s)
c103c5-s2	656.58	0.17	656.58	0.04
c206c5-s4	960.03	0.23	960.03	0.05
c208c5-s3	626.90	0.25	626.90	0.05
r202c5-s3	517.30	0.64	517.30	0.04
r203c5-s4	696.69	0.53	696.69	0.04
rc204c5-s4*	713.66	2.52	713.66	0.04
rc208c5-s3	656.67	0.97	656.67	0.03
c202c10-s5	1157.38	5.43	1157.38	0.07
r201c10-s4	942.12	32.29	942.12	0.08
r203c10-s5	871.55	7200.00	871.55	0.08
rc201c10-s4	1635.78	0.7	1635.78	0.07
r209c15-s5	1366.20	7200.00	**1232.64**	0.28
rc204c15-s7	1700.47	7200.00	**1475.92**	0.43
Average	961.64	1664.90	934.09	0.10

*Initial tour is randomly constructed to obtain the optimal solution

6.4. Effect of Battery Degradation

In this section, we investigate the effect of battery degradation on route plans and costs by comparing ETSPTW and ETSPTW-BD results obtained with MatHeur. 25 runs were performed for each instance of the modified benchmark dataset of Roberti and Wen (2016), and the best achieved solution and average runtimes are reported. Note that the cost calculations of ETSPTW solutions are made by assuming that the EVs depart from the depot as fully charged since this is a common practice in the industry.

Table 6.6. Effect of battery degradation on small-size instances with 5-stations

	ETSPTW			ETSPTW-BD			
Instance	Cost	t (s)	#R	Cost	t (s)	#R	%Δ
n20w120s5.1	1114.28	0.54	4	1021.63	0.81	6	8.31
n20w120s5.2	933.63	0.63	3	875.39	0.53	5	6.24
n20w120s5.3	1205.80	0.29	3	1190.44	0.41	5	1.27
n20w120s5.4	1239.07	0.23	4	1175.12	0.42	6	5.16
n20w120s5.5	1008.12	0.25	3	975.21	0.45	5	3.26
n20w140s5.1	760.94	0.20	3	710.51	0.19	5	6.63
n20w140s5.2	1130.90	0.27	2	1067.26	0.43	7	5.63
n20w140s5.3	972.20	0.13	3	909.55	0.15	6	6.44
n20w140s5.4	1047.96	0.64	3	1024.95	0.29	4	2.20
n20w140s5.5	906.18	0.34	3	868.65	0.26	6	4.14
n20w160s5.1	977.65	0.31	3	924.46	0.56	5	5.44
n20w160s5.2	878.69	0.45	4	848.71	0.39	4	3.41
n20w160s5.3	887.50	0.28	3	838.45	0.34	4	5.53
n20w160s5.4	862.54	0.30	3	798.92	0.52	5	7.38
n20w160s5.5	1043.10	0.60	3	991.81	0.74	4	4.92
n20w180s5.1	1077.01	0.25	3	1000.49	0.45	6	7.10
n20w180s5.2	1108.33	0.37	3	1065.46	0.57	5	3.87
n20w180s5.3	1108.57	0.26	3	1059.81	0.44	5	4.40
n20w180s5.4	823.09	0.32	3	788.39	0.55	4	4.22
n20w180s5.5	831.34	0.43	3	798.85	0.75	4	3.91
n20w200s5.1	935.90	0.22	3	924.49	0.45	4	1.22
n20w200s5.2	879.79	0.26	4	839.75	0.47	5	4.55
n20w200s5.3	994.31	0.33	4	953.70	0.43	4	4.08
n20w200s5.4	1239.10	0.42	3	1130.32	0.55	5	8.78
n20w200s5.5	969.71	0.47	4	926.50	0.65	6	4.46
Average	997.43	0.35	3.20	948.35	0.47	5.00	4.90

6.4.1. Results for Small-Size Instances

In this subsection, we make comparisons over the problem instances with 20-customers. We run MatHeur by setting *#NonImpIter* and *CL Size* to 4*n* and *n*, respectively since the

problem sizes are small. Furthermore, local optimum solutions obtained after each LS operator are sent to the FTVCP phase. Table 6.6 and Table 6.7 show the results obtained for the instances with 5- and 10-stations, respectively. In these tables 'Cost' refers to the total cost of energy consumption plus battery degradation costs of the best tour obtained through runs. We should note that in the cost calculation under 'ETSPTW' we considered the optimal solutions presented in Section 6.3.2, and the corresponding total cost is the realized cost with battery degradation effect. Column '#R' indicates the number of recharges along tours. '%Δ' reports the percentage difference between the cost of the best solutions obtained with MatHeur in the context of the ETSPTW and ETSPTW-BD.

Table 6.7. Effect of battery degradation on small-size instances with 10-stations

	ETSPTW			ETSPTW-BD			
Instance	Cost	t (s)	#R	Cost	t (s)	#R	%Δ
n20w120s10.1	1131.02	0.66	3	1006.83	0.84	7	10.98
n20w120s10.2	894.67	0.63	3	843.69	0.76	5	5.70
n20w120s10.3	1195.92	0.24	3	1171.81	0.44	6	2.02
n20w120s10.4	1208.16	0.53	3	1139.19	0.42	6	5.71
n20w120s10.5	982.46	0.33	3	938.98	0.55	6	4.43
n20w140s10.1	742.03	0.21	4	697.28	0.42	5	6.03
n20w140s10.2	1035.52	0.32	3	1034.69	0.45	4	0.08
n20w140s10.3	955.22	0.16	4	895.38	0.16	8	6.26
n20w140s10.4	998.63	0.53	3	974.70	0.32	6	2.40
n20w140s10.5	924.44	0.33	3	850.57	0.34	7	7.99
n20w160s10.1	977.65	0.43	3	914.81	0.69	6	6.43
n20w160s10.2	880.95	0.60	3	828.46	0.59	4	5.96
n20w160s10.3	887.50	0.31	3	815.40	0.37	6	8.12
n20w160s10.4	862.54	0.32	3	798.26	0.54	5	7.45
n20w160s10.5	999.96	0.50	3	958.17	1.01	6	4.18
n20w180s10.1	1029.07	0.24	3	967.15	0.58	7	6.02
n20w180s10.2	1127.32	0.39	3	1051.89	0.54	6	6.69
n20w180s10.3	1136.74	0.27	4	1046.90	0.56	6	7.90
n20w180s10.4	803.08	0.31	3	768.38	0.73	4	4.32
n20w180s10.5	817.87	0.41	3	780.34	1.06	6	4.59
n20w200s10.1	935.90	0.24	3	897.41	0.72	7	4.11
n20w200s10.2	863.16	0.25	4	815.74	0.53	5	5.49
n20w200s10.3	975.16	0.33	4	928.44	0.77	6	4.79
n20w200s10.4	1228.18	0.46	5	1107.15	0.72	7	9.85
n20w200s10.5	971.62	0.50	3	909.83	1.11	7	6.36
Average	982.59	0.38	3.28	925.66	0.61	5.92	5.75

Significant amounts of cost savings are obtained in all problem instances when battery degradation is taken into account. The average cost savings are 4.90% and 5.75% in the

instances with 5- and 10-stations, respectively, while it can reach up to 10.98%. The cost-saving becomes higher as the number of existing recharging facilities increases. The results also show that incorporating battery degradation leads to more frequent recharges en route. The average increases in the number of recharging visits are 56% and 80% in the instances with 5- and 10-stations, respectively. This is an expected result due to the non-decreasing wear cost function where lower SOC intervals are more preferable. Hence, the recharge frequency, amount of energy transferred and sequence of customers are determined based on the trade-off between energy consumption (distance) and wear costs. Even though the computational times are not long, the runtimes rise by 34% and 61% in the instances with 5- and 10-stations, respectively when the battery degradation is considered.

Table 6.8. Effect of battery degradation on large-size instances with 5-stations

	ETSPTW			ETSPTW-BD			
Instance	Cost	t (s)	#R	Cost	t (s)	#R	%Δ
n150w120s5.1	3163.53	28.36	7	2946.55	31.00	12	6.86
n150w120s5.2	2629.22	21.92	6	2519.96	39.12	9	4.16
n150w120s5.3	3186.59	18.24	8	3176.46	19.44	8	0.32
n150w120s5.4	2791.63	23.28	7	2704.49	29.20	9	3.12
n150w120s5.5	2892.34	21.56	9	2763.56	40.84	13	4.45
n150w140s5.1	3048.80	30.44	8	2917.76	41.00	11	4.30
n150w140s5.2	3100.06	21.96	8	2986.75	37.64	12	3.66
n150w140s5.3	2547.36	23.28	7	2434.18	39.56	11	4.44
n150w140s5.4	2758.18	17.32	8	2630.78	25.40	13	4.62
n150w140s5.5	2622.80	30.80	7	2545.28	38.16	11	2.96
n150w160s5.1	3026.75	22.68	7	2819.10	27.84	10	6.86
n150w160s5.2	2920.03	31.48	7	2832.41	41.20	11	3.00
n150w160s5.3	2418.35	18.32	7	2376.24	25.84	10	1.74
n150w160s5.4	2785.13	23.40	7	2700.12	25.48	10	3.05
n150w160s5.5	2781.62	27.28	7	2629.97	43.44	12	5.45
n200w120s5.1	2997.13	53.28	6	2882.18	94.40	8	3.84
n200w120s5.2	3059.62	62.24	9	2894.23	72.08	12	5.41
n200w120s5.3	3429.22	62.24	8	3282.02	78.64	12	4.29
n200w120s5.4	3391.19	62.00	7	3234.27	65.76	11	4.63
n200w120s5.5	3278.67	53.48	7	3135.87	71.36	10	4.36
n200w140s5.1	3299.12	85.92	7	3146.56	102.96	10	4.62
n200w140s5.2	3243.97	73.48	8	3121.76	96.44	12	3.77
n200w140s5.3	2988.91	53.48	8	2852.66	63.40	11	4.56
n200w140s5.4	3120.22	83.88	8	2977.19	107.20	10	4.58
n200w140s5.5	3304.51	54.76	8	3204.75	73.68	11	3.02
Average	2991.40	40.20	7.44	2868.60	53.24	10.76	4.08

6.4.2. Results for Large-Size Instances

We compare the solutions obtained for 150- and 200-customer instances in this subsection. The algorithm is executed with the parameter values found in Section 6.2. Since the problem sizes are large, the tours found in the earlier phases of MatHeur are not good candidates for inserting the charge stations. Hence, the FTVCP is not solved for the solutions found within the first $n/5$ iterations of MatHeur. The results for the instances with 5 and 10 charging stations are presented in Table 6.8 and Table 6.9, respectively. We should note that the objective of the ETSPTW is simply the minimization of energy consumption, and the cost of the tour is calculated by considering the battery wear cost.

Table 6.9. Effect of battery degradation on large-size instances with 10-stations

	ETSPTW			ETSPTW-BD			
Instance	Cost	t (s)	#R	Cost	t (s)	#R	%Δ
n150w120s10.1	3066.87	28.56	7	2882.64	34.68	14	6.01
n150w120s10.2	2619.78	21.88	6	2472.51	39.00	11	5.62
n150w120s10.3	3173.32	18.96	8	3156.89	21.16	11	0.52
n150w120s10.4	2809.94	23.04	6	2632.86	30.40	13	6.30
n150w120s10.5	2844.28	20.92	8	2635.41	41.12	15	7.34
n150w140s10.1	3049.03	29.88	8	2845.26	41.24	14	6.68
n150w140s10.2	3096.72	22.00	7	2917.03	37.72	13	5.80
n150w140s10.3	2544.59	23.76	8	2403.06	50.88	12	5.56
n150w140s10.4	2747.57	17.32	8	2580.90	23.00	16	6.07
n150w140s10.5	2580.34	30.76	7	2474.20	37.96	14	4.11
n150w160s10.1	2929.22	21.96	7	2749.64	36.04	14	6.13
n150w160s10.2	2849.93	31.64	7	2739.07	41.24	10	3.89
n150w160s10.3	2412.05	18.56	7	2317.31	26.84	11	3.93
n150w160s10.4	2808.89	23.44	7	2648.12	25.00	15	5.72
n150w160s10.5	2678.73	27.08	8	2564.83	46.96	10	4.25
n200w120s10.1	3032.07	52.52	6	2822.28	94.00	10	6.92
n200w120s10.2	2998.27	62.24	9	2831.05	73.56	14	5.58
n200w120s10.3	3371.26	62.36	8	3184.87	79.24	13	5.53
n200w120s10.4	3344.27	62.00	8	3126.69	64.04	14	6.51
n200w120s10.5	3207.94	53.52	8	3052.36	58.08	15	4.85
n200w140s10.1	3290.84	86.00	7	3094.30	102.36	13	5.97
n200w140s10.2	3211.71	71.48	7	3057.77	99.80	12	4.79
n200w140s10.3	2930.87	53.52	9	2811.51	66.44	12	4.07
n200w140s10.4	3162.53	83.84	8	2960.55	112.64	12	6.39
n200w140s10.5	3377.51	54.84	7	3164.25	75.96	12	6.31
Average	2965.54	40.08	7.44	2805.01	54.37	12.80	5.39

As in Section 6.4.1, the total cost is improved when battery wear is considered in all

problem instances. In the instances with 5-stations, the average cost improvement is 4.08% and the savings can be as large as 6.86%. In the instances with 10-stations, the total cost can be reduced by 5.39% on average and cost improvement may rise to 7.34%. Furthermore, the availability of charging stations contributes more when the battery degradation is concerned. When the number of charging stations is increased from 5 to 10, the average cost decreases by 0.86% in the ETSPTW setting whereas this rate is 1.31% in the ETSPTW-BD setting. The consideration of battery wear costs increases the recharging frequency along the tour, where the number of recharges increases by 44% and 72% on average in the instances with 5- and 10-stations, respectively. Although the length of the tours becomes longer because of the more detours and changes in the customer sequences, better recharging plans result in less battery degradation cost and hence cause saving in total operational cost. On the other hand, incorporating the battery degradation brings additional complexity to the problem, and the computational times required to obtain a solution increase by 32% and 35% in the instances with 5- and 10-stations, respectively.

6.5. Trade-off Analysis

In this section, we perform sensitivity analyses based on the parameters of the problem instances, and a trade-off analysis by devising a multi-start version of MatHeur. The sensitivity analyses are only performed on the instances which are used during the parameter tuning, and the comparisons are based on the best results achieved.

6.5.1. The Effect of Battery Capacity

We observed in Section 6.4 that recharging frequencies along the tours significantly increase when the battery degradation is considered. Therefore, we increase the battery sizes of the EVs in each problem instance by 25% and 50%, separately to examine the impact of increased battery capacities on the solutions. We compare the solutions obtained for these 2 new cases with the ones presented in Section 6.4.2. Table 6.10 summarizes the results with respect to the percentage change in total operational cost and the difference in the number of recharges en route. A negative value under ‘ΔCost(%)’ and ‘Δ#R’ indicate a cost-saving and a decrease in the number of recharging visits, respectively whereas ‘-‘ means no change. As the battery capacity increases, the need for recharging en route decreases, and this results in fewer detours, a decrease in the route

length and less energy consumption. Hence, the total operational cost is also reduced.

Table 6.10. Comparisons of results with respect to increased battery capacities

	25%		50%	
Instance	ΔCost (%)	Δ#R	ΔCost (%)	Δ#R
n150w120s5.2	-1.96	-	-2.87	-
n150w140s5.1	-2.02	-2	-3.17	-3
n150w140s5.4	-1.96	-1	-2.86	-2
n150w160s5.2	-4.84	-3	-7.00	-3
n150w160s5.3	-3.58	-3	-5.03	-3
n200w120s5.1	-2.11	-	-3.28	-
n200w120s5.4	-1.98	-2	-3.53	-3
n200w120s5.5	-1.49	-1	-2.40	-1
n200w140s5.3	-1.67	-	-2.84	-2
n200w140s5.4	-1.63	-	-2.67	-2
Average	-2.32	-1.20	-3.57	-1.90

6.5.2. The Effect of Time Windows

We repeat our experiments by extending the time windows of customer nodes by keeping the the length of planning horizon the same to explore the effects of time windows on the route and recharging plans made while considering battery degradation. We obtain the results by increasing the late arrival times of customer nodes by 50% of their time window width and without imposing any time windows restriction within the planning horizon, separately. Table 6.11 presents the comparative results. A positive value under 'Δ#R' indicate an increase in the number of recharging visits.

Table 6.11. Comparisons of results obtained with respect to extended time windows

	50%		No TW	
Instance	ΔCost (%)	Δ#R	ΔCost (%)	Δ#R
n150w120s5.2	-2.58	1	-28.89	-3
n150w140s5.1	-7.23	-	-38.09	-5
n150w140s5.4	-3.07	-1	-31.19	-5
n150w160s5.2	-11.28	-2	-35.44	-5
n150w160s5.3	-2.78	-	-22.14	-3
n200w120s5.1	-7.39	-	-27.12	-1
n200w120s5.4	-8.26	-1	-35.92	-5
n200w120s5.5	-7.62	-1	-33.34	-5
n200w140s5.3	-6.68	-1	-27.75	-5
n200w140s5.4	-7.65	1	-32.17	-3
Average	-6.45	-0.4	-31.21	-4.0

The saving in the operational cost increases as the time window restrictions are relaxed since the options for consecutive visits of closer customers in the route increase. The number of recharges along the tour significantly decreases when no time windows constraints are imposed whereas it reduces by only 3.85% even if the time windows are extended by 50%. As observed in Sections 6.4.1 and 6.4.2, the number of recharges en route significantly increased when battery degradation is considered, and this finding still holds with looser time windows.

6.5.3. Multi-Start Solution Strategy

In our experiments, we observed that the deviations between the best and average results found by MatHeur can be large in some instances. Thus, we designed a multi-start version of MatHeur to investigate the trade-off between the solution quality and run time. In the multi-start version, a new tour is constructed after *#NonImpIter* is reached if *#Iter* is not exceeded. *#Iter* is set to $5n$ instead of $4n$ while the remaining parameters remain unchanged. The number of runs performed for each problem instance is limited to 10. The phase of solving the FTVCP is not performed during the first $n/5$ iterations.

We compare the results obtained with the single- and multi-start versions of MatHeur in Table 6.12. We grouped the instances according to the time windows width and the number of charging stations. Hence, we obtained 10 separate subsets with 5 instances in each. Table 6.12 report the results for the subsets whereas the detailed results can be found in Appendix B. The group of instances is given under column 'Subset'. 'Best' reports the average of the best results found in 5 instances of the subset whereas 'Avg' stands for the average of the average solutions. '%Dev' shows the percentage deviation of the average OFV from the best OFV.

Although the best solutions achieved by the two versions are similar, the convergence of the algorithm improves with the multi-start version even if it remains at a high level in some instances due to Slack. On the other hand, the total runtime increases by 31% when the number of runs for the versions is considered which are 25 and 10 in the single- and multi-start versions, respectively.

Table 6.12. Comparison of single- and multi-start strategies

	Single-start				Multi-start			
Subset	Best	Avg	%Dev	t (s)	Best	Avg	%Dev	t (s)
n150w120s5	2822.20	2865.78	1.58	31.92	2809.50	2848.00	1.33	112.92
n150w140s5	2702.95	2763.33	2.21	36.35	2697.92	2722.83	0.94	122.40
n150w160s5	2671.57	2750.81	2.91	32.76	2679.78	2715.51	1.31	103.26
n200w120s5	3085.71	3161.36	2.51	76.45	3078.36	3118.28	1.32	260.76
n200w140s5	3060.58	3189.13	4.24	88.74	3077.54	3128.80	1.68	273.62
n150w120s10	2756.06	2794.98	1.45	33.27	2732.63	2766.41	1.18	119.18
n150w140s10	2644.09	2702.22	2.16	38.16	2641.43	2662.10	0.78	126.16
n150w160s10	2603.79	2695.55	3.45	35.22	2611.18	2665.19	2.02	112.68
n200w120s10	3003.45	3077.94	2.52	73.78	3000.66	3034.52	1.14	249.32
n200w140s10	3017.68	3138.69	4.05	91.44	3031.50	3078.32	1.55	281.26
Average	2836.81	2913.98	2.71	53.81	2836.05	2874.00	1.33	176.16

7. THE ELECTRIC VEHICLE ROUTING PROBLEM WITH TIME WINDOWS BY CONSIDERING BATTERY DEGRADATION

In this chapter, we address the EVRPTW in which customers' demands are met by a homogenous fleet of EVs within specified time windows by considering service times. Furthermore, partial recharging is allowed, and its duration is assumed to be linearly proportional to the amount of energy transferred during the recharging by assuming that the EV is operated between 10% to 90% of its battery capacity which is a practical action taken by LSPs (Pelletier et al., 2017). In addition, there is a one-to-one relationship between energy consumed and distance traveled. Finally, only one recharging visit is permitted between two consecutive customers since it is highly observed in urban logistics operations. As in Chapter 4, we still utilize the modeling approach of Pelletier et al. (2018) to represent the influence of battery wear on the route and charge schedules of EVs and consider a non-decreasing wear cost function.

7.1. Mathemaical Model

For the sake of completeness and ease of understanding, we provide the whole mathematical notation. We follow the notation used in Rastani et al. (2019) and Bruglieri et al. (2016). Let $V = \{1, \dots, n\}$ denote the set of customers, *K* denote the set of EVs, and F denote the set of charging stations. Each vehicle departs from node 0 and returns to node $n + 1$ at the end of its trip where both nodes denote the same depot. We define $V_0 = V \cup \{0\}$, $V_{n+1} = V \cup \{n + 1\}$ and $V_{0,n+1} = V \cup \{0, n + 1\}$. Now, the problem can be defined on a complete directed graph $G = (N, A)$ in which $A = \{(i, j) | i, j \in N, i \neq j\}$ is the set of arcs and $N = V_{0,n+1} \cup F$ is the set of all nodes on the network.

Each customer $i \in V$ has a demand of q_i, service time of s_i, and time window of $[e_i, l_i]$.

Since the fleet is homogenous, all EVs have the same load capacity of C and operational battery capacity of Q. At a charging station, one unit of energy is charged in g time units. The direct distance from customer i to customer j is denoted by d_{ij} while $\hat{d}_{ijs} = d_{is} + d_{sj} - d_{ij}$ corresponds to the additional distance if the vehicle is recharged at station s en route. Likewise, t_{ij} denotes the direct travel time from customer i to customer j, and $\hat{t}_{ijs} = t_{is} + t_{sj} - t_{ij}$ is the additional travel time if there is a recharging visit in between customers i and j at station s. However, $\hat{t}_{ijs}$ does not involve the recharging time at station s. In addition, the energy is consumed by the rate of h^d for each unit of distance. Hence, the total energy needed to directly move from customer i to customer j is calculated as $h_{ij} = h^d d_{ij}$ which is a linear function of the distance. If a recharging visit takes place at station s during the move between customer i and customer j, the calculation of additional energy consumption is as follows: $\hat{h}_{ijs} = h_{is} + h_{sj} - h_{ij}$. The set D and parameters LB^d, UB^d, L and W^d are already defined in Sections 3 and 4.2.

The decision variables y_i^k keep track of the battery SOC of the vehicle k when it arrives at customer/depot $i \in V_{0,n+1}$. On the other side, decision variables y_{ijs}^k and Y_{ijs}^k take values when there is a recharging visit at station $s \in F$ on route (i, s, j), $i \in V_0, j \in V_{n+1}$, and represents the battery SOC at arrival to and departure from the charging station s, respectively. The decision variable τ_i represents the service starting time at any node $i \in N$. The binary decision variable x_{ij}^k is 1 if the arc (i, j) is traversed by the vehicle k, $i \in V_0$, $j \in V_{n+1}$ and 0 otherwise. The binary decision variable z_{ijs}^k takes value 1 when the vehicle k travels from node $i \in V_0$ to node $j \in V_{n+1}$ via station $s \in F$ and 0 otherwise. The decision variables and the constraints are categorized into two as ones that belong to stations and ones that belong to the depot for overnight recharging to better express the battery degradation characteristics as follows: The decision variables soc_{ijd}^k and soc_d^k keep track of how much the portion of SOC interval $d \in D$ is utilized during the recharging at a station and the depot, respectively. The binary decision variables u_{ijd}^k and u_d^k take value 1 if the SOC interval $d \in D$ is used to charge the vehicle $k \in K$ at a charging station and at the depot, respectively; and 0 otherwise. Remember since only one recharging visit is allowed between two consecutive customers there is no need for the indication of a charging station index in these decision variables. Furthermore, the vehicle is assumed to be initially charged with the amount of the difference between the battery

SOC when it departs from the depot and arrives at the depot since that much energy is consumed during the route. Finally, the EV will have consumed its whole operational battery capacity when it returns to the depot due to the non-decreasing wear cost function if it has been recharged at least once en route.

The mathematical notation associated with the EVRPTW-BD formulation is presented in Table 7.1. In what follows, the 0-1 mixed-integer linear programming model of the problem is formulated.

Table 7.1. Mathematical notation of EVRPTW-BD

Sets	
V	Set of customers
V_0	Set of customers and departure depot
V_{n+1}	Set of customers and arrival depot
$V_{0,n+1}$	Set of customers, departure and arrival depots
F	Set of charging stations
N	Set of customers, stations and depots
K	Set of vehicles
D	Set of SOC intervals
Parameters	
d_{ij}	Distance between node i and j
$\hat{d}_{ijs}$	Additional distance of visiting station s between customers i and j, $\hat{d}_{ijs} = d_{is} + d_{sj} - d_{ij}$
t_{ij}	Travel time from node i to node j
$\hat{t}_{ijs}$	Additional travel time of visiting station s between customers i and j, $\hat{t}_{ijs} = t_{is} + t_{sj} - t_{ij}$
q_i	Demand of customer i
r_i	Service time of customer i
$[e_i, l_i]$	Time window of customer i
l_0	Length of the planning horizion
C	Load capacity
Q	Operational battery capacity
g	Recharging rate
h_{ij}	Total energy consumed to traverse arc (i, j)
$\hat{h}_{ijs}$	Additional consumption if the vehicle is recharged in station s while traveling from customer i to customer j, $\hat{h}_{ijs} = h_{is} + h_{sj} - h_{ij}$
c	Unit energy cost
W^d	Wear cost per unit energy charged or discharged within the SOC interval d
L	Length of SOC intervals
UB^d	Upper SOC bound of interval d
LB^d	Lower SOC bound of interval d
Decision variables	
τ_i	Service starting time at customer $i \in V$
y_i^k	Battery SOC of vehicle $k \in K$ upon arrival at (departure from) customer (depot) $i \in$

$V_{0,n+1}$

y_{ijs}^k Battery SOC of vehicle $k \in K$ upon arrival at station $s \in F$ on route (i,s,j), $i \in V_0, j \in V_{n+1}$

Y_{ijs}^k Battery SOC of vehicle $k \in K$ at the departure from station $s \in F$ on route (i,s,j), $i \in V_0, j \in V_{n+1}$

soc_{ijd}^k Portion of SOC interval $d \in D$ used during the charging of vehicle $k \in K$ at station $s \in F$ on route (i,s,j), $i \in V_0, j \in V_{n+1}$

soc_d^k Portion of SOC interval $d \in D$ used during the overnight charging of vehicle $k \in K$ at the depot

x_{ij}^k 1 if vehicle $k \in K$ travels from node $i \in V_0$ to node $j \in V_{n+1}$; 0 otherwise

z_{ijs}^k 1 if vehicle $k \in K$ traverses arc (i,j), $i \in V_0, j \in V_{n+1}$, through station $s \in F$; 0 otherwise

u_{ijd}^k 1 if interval $d \in D$ is used to charge vehicle $k \in K$ at station $s \in F$ on route (i,s,j), $i \in V_0, j \in V_{n+1}$; 0 otherwise

u_d^k 1 if interval $d \in D$ is used to charge vehicle $k \in K$ at the depot; 0 otherwise

$$\text{Min } c\left(\sum_{i\in V_0}\sum_{j\in V_{n+1}}\sum_{s\in F}\sum_{k\in K}(Y_{ijs}^k - y_{ijs}^k)\right) + c\left(\sum_{k\in K} y_0^k - y_{n+1}^k\right) \tag{7.1.1}$$

$$+Q\left(\sum_{i\in V_0}\sum_{j\in V_{n+1}}\sum_{k\in K}\sum_{d\in D} W^d soc_{ijd}^k\right) + Q\left(\sum_{d\in D}\sum_{k\in K} W^d soc_d^k\right) \tag{7.1.2}$$

Subject to

$$y_0^k = Q \qquad \forall k \in K \tag{7.2}$$

$$\sum_{\substack{j\in V_{n+1}\\ i\neq j}}\sum_{k\in K} x_{ij}^k = 1 \qquad \forall i \in V \tag{7.3}$$

$$\sum_{\substack{i\in V_0\\ i\neq j}} x_{ij}^k - \sum_{\substack{i\in V_{n+1}\\ i\neq j}} x_{ji}^k = 0 \qquad \forall j \in V, \forall k \in K \tag{7.4}$$

$$\sum_{s\in F} z_{ijs}^k \leq x_{ij}^k \qquad \forall i \in V_0, \forall j \in V_{n+1}, \forall k \in K, i \neq j \tag{7.5}$$

$$\tau_i + (t_{ij} + r_i)x_{ij}^k + \sum_{s\in F}(\hat{t}_{ijs} z_{ijs}^k + g(Y_{ijs}^k - y_{ijs}^k)) - l_0(1 - x_{ij}^k) \leq \tau_j \qquad \forall i \in V_0, \forall j \in V_{n+1}, \forall k \in K, i \neq j \tag{7.6}$$

$$e_j \leq \tau_j \leq l_j \qquad \forall j \in N \tag{7.7}$$

$$\sum_{i \in V} \sum_{j \in V_{n+1}} q_i x_{ij}^k \leq C \qquad \forall k \in K \qquad (7.8)$$

$$0 \leq y_j^k \leq y_i^k - h_{ij} x_{ij}^k + Q(1 - x_{ij}^k + \sum_{s \in F} z_{ijs}^k) \qquad \forall i \in V_0, \forall j \in V_{n+1}, \forall k \in K, i \neq j \qquad (7.9)$$

$$y_j^k \leq \sum_{s \in F} (Y_{ijs}^k - h_{sj} z_{ijs}^k) + Q\left(1 - \sum_{s \in F} z_{ijs}^k\right) + Q(1 - x_{ij}^k) \qquad \forall i \in V_0, \forall j \in V_{n+1}, \forall k \in K, i \neq j \qquad (7.10)$$

$$0 \leq y_{ijs}^k \leq y_i^k - h_{is} z_{ijs}^k + Q(1 - x_{ij}^k) \qquad \forall i \in V_0, \forall j \in V_{n+1}, \forall s \in F, \forall k \in K, i \neq j \qquad (7.11)$$

$$y_{ijs}^k \leq Y_{ijs}^k \leq Q z_{ijs}^k \qquad \forall i \in V_0, \forall j \in V_{n+1}, \forall s \in F, \forall k \in K, i \neq j \qquad (7.12)$$

$$Q \sum_{d \in \mathrm{D}} soc_{ijd}^k = \sum_{s \in \mathrm{F}} (Y_{ijs}^k - y_{ijs}^k) \qquad \forall i \in V_0, \forall j \in V_{n+1}, \forall k \in K, i \neq j \qquad (7.13)$$

$$Q \sum_{d \in \mathrm{D}} soc_d^k = y_0^k - y_{n+1}^k \qquad \forall k \in K \qquad (7.14)$$

$$0 \leq soc_{ijd}^k \leq L.u_{ijd}^k \qquad \forall i \in V_0, \forall j \in V_{n+1}, \forall d \in D, \forall k \in K, i \neq j \qquad (7.15)$$

$$0 \leq soc_d^k \leq L.u_d^k \qquad \forall d \in D, \forall k \in K \qquad (7.16)$$

$$Q.soc_{ijd}^k \leq Q.UB^d - \sum_{s \in \mathrm{F}} y_{ijs}^k + Q(1 - u_{ijd}^k) \qquad \forall i \in V_0, \forall j \in V_{n+1}, \forall d \in D, \forall k \in K, i \neq j \qquad (7.17)$$

$$Q.soc_d^k \leq Q.UB^d - y_{n+1}^k + Q(1 - u_d^k) \qquad \forall d \in D, \forall k \in K \qquad (7.18)$$

$$x_{ij}^k \in \{0,1\} \qquad \forall i \in V_0, \forall j \in V_{n+1}, \forall k \in K \qquad (7.19)$$

$$z_{ijs}^k \in \{0,1\} \qquad \forall i \in V_0, \forall j \in V_{n+1}, \forall s \in F, \forall k \in K \qquad (7.20)$$

$$u_d^k \in \{0,1\} \qquad \forall d \in D, \forall k \in K \qquad (7.21)$$

$$u_{ijd}^{k} \in \{0,1\} \qquad \forall i \in V_0, \forall j \in V_{n+1}, \forall d \, \forall D, \forall k \in K \qquad (7.22)$$

The objective function (7.1.1) of the model minimizes the total energy and battery degradation costs. The expression (7.1.1) corresponds to total energy consumption by considering the energy amount that is transferred at charging stations and the depot, respectively whereas the expression (7.1.1) represents the battery degradation costs incurred during the recharges at charging stations and the depot, respectively. The initial battery SOC of the EVs during their departure is set to full by constraints (7.2). Constraints (7.3) ensure connectivity between customers. Constraints (7.4) enforce that each customer is visited only once. Constraints (7.5) make sure that recharging the battery en route is only possible if there is a trip from customer i to j. The time feasibility of arcs emanating from the customers and the depot is guaranteed by constraints (7.6). Constraints (7.7) ensure that each customer is served in its time window. By the way, Constraints (7.6)–(7.7) eliminate the sub-tours. Constraints (7.8) guarantee the load of the vehicles can not exceed the cargo capacity during the trip. Constraints (7.9)–(7.11) keep track of the battery SOC at each node and ensure that it never falls below zero. Constraints (7.9) establish this relation when the vehicle directly travels from customer i to customer j without recharging en route. On the other side, constraints (7.10)–(7.11) provide the battery SOC consistency if the vehicle recharges itself when moving from customer i to customer j: constraints (7.10) set the battery SOC during the arrival at customer j whereas constraints (7.11) determine the SOC level during the arrival at a station. Constraints (7.12) make sure that the battery SOC during the departure from a station remains in a certain interval, i.e. it can not be larger than the amount during its arrival at the station and exceed the battery capacity. Constraints (7.13)–(7.14) equalize the difference between the energy levels when arriving at a charging station (the depot) and departing from that charging station (the depot) to the sum of energy charged over all SOC intervals. Constraints (7.15)–(7.16) set limits on the utilization of SOC intervals for the recharges at stations and the depot, respectively. These constraints ensure that an SOC interval is nonnegative and can not exceed its length. Constraints (7.17)–(7.18) make sure that SOC intervals can take a positive value if the battery SOC during the arrival at the station and the depot is less than the upper bound of the corresponding SOC interval; and enforce that SOC intervals take the value 0 if the upper bound of the related SOC interval is

already lower than the battery SOC of the vehicle during its arrival at the station and the depot, respectively. These constraints are a must since the wear cost function is non-decreasing, i.e. the solution found by solving the model tends to fill lower SOC intervals that are cheaper. Finally, constraints (7.19)–(7.22) define the binary decision variables.

7.2. Experimental Study

7.2.1. Experimental Design

We conduct experimental tests on the EVRPTW benchmark instances devised by Schneider et al. (2014). 36 small and 56 large data instances exist in this dataset. Since large problems are intractable, we practice on small-size instances. There are three subsets within this dataset, which have 5, 10 and 15 customers, respectively: each with 12 distinct problems. In addition, customers are characterized with respect to the initial letter(s) of the problem. Customers are either clustered (C) or randomly scattered (R) or both clustered and randomly (RC) scattered on a map. These three subsets are also divided into two subsets which are observable through the 3-digit number in the nomenclatures as the ones starting with 1 and 2, respectively. This further branching yields different time window lengths and capacities for the battery and cargo load. In the nomenclature of the problem instances, finally, the number beside 's' corresponds to the number of charging stations available in this dataset. For example, the instance 'c101c5-s3' contains 5 clustered customers and 3 charging stations.

We set h^d to 1, i.e. traveling one unit of distance requires one unit of energy, and c to 1. The parameters related to battery degradation are the same as explained in Section 6.1.

We performed our experiments using three different scenarios. In Scenario 1, we considered the optimal (or best-known) solutions reported in Keskin and Çatay (2016) and Rastani et al. (2019) and calculated the corresponding total cost by taking into account battery wear cost. In Scenario 2, we solved the model presented in Section 7.1. Finally, in Scenario 3, we repeated Scenario 2 by relaxing constraint (7.2) which enforces the EV to depart from the depot fully charged. In other words, the initial energy level of the battery becomes a decision variable. We aim not only to investigate the possible benefits of considering wear cost besides the energy cost but also to measure its additional complexity in terms of computational time. We obtained the solutions by using IBM ILOG CPLEX version 12.9.0 on a Windows 10 OS computer with an Intel i7-8700 3.20

GHz CPU and 32 GB RAM. CPLEX was run in the default mode with a computing time limit of 10 hours.

7.2.2. Numerical Results

We could solve all 5-customer problem instances at optimality. That's why, we did not report any optimality gap for these solutions. The results are provided in Table 7.2. The nomenclature of the problem instances is shown under the first column. The columns '*EC*', '*WC*' and '*TC*' refer to the energy cost, wear cost and total cost of the route, respectively. The number of recharges en route is reported under column '#*R*' and column '*t (sec)*' shows the computational time required for each scenario in seconds. The last two columns evaluate the percentage cost differences between scenarios 1-2 and 1-3, respectively, and a positive value indicates cost saving. Noting that '*EC*' also reports the total distance traveled, we show the increase in route lengths in italic. We indicated improvements in total costs in bold. 5 out of 12 and 6 out of 12 routes become longer in the second and third scenarios, respectively because of more frequent recharging visits. This increase in the frequency of recharging is simply due to the non-decreasing wear cost function where utilizing lower SOC intervals is preferable since wear cost increases in the higher SOC intervals. Hence, the battery is recharged as much as needed more frequently. An average of 5.2% improvement in total cost is obtainable by considering the improvement from the third scenario. Hence, this demonstrates that optimizing overnight charging at the depot can bring additional cost savings. Finally, run times did not increase significantly.

We presented the solutions for 10-customer instances in Table 7.3. We could not find the optimal solution for two problem instances in 10 hours in scenarios 2 and 3. An inferior upper bound is provided by CPLEX in one of the problem instances in scenario 2 due to the complexity of the problem. We should note that the solutions in the first scenario are already feasible solutions for the second and the third scenarios as well. Route plans change in 5 and 9 out of 12 problem instances for the second and third scenarios, respectively. The average improvement in total cost is 3.4% while the third setting again contributes more significantly. Besides not being able to find the optimal solutions in two instances, the run times increased dramatically.

We reported the solutions for 15-customer instances in Table 7.4. CPLEX used the entire time allocated for each problem instance in the second and third scenarios, and the

optimality of the solutions was not guaranteed. Hence, we only provide the statistics for optimality gaps. In addition, CPLEX could not find even a feasible solution in one of the problem instances in both the second and third scenarios. As indicated with negative percentage deviations in the last two columns, inferior upper bounds are provided by CPLEX in some of the problem instances for the second and third scenarios. Excluding these instances, we observe that the total cost can be reduced by 5.7% on average and the savings can be as large as 9.9%. These results reveal the potential benefits of considering the battery wear explicitly when making the routing decisions.

Table 7.2. Results for 5-customer instances

	Scenario 1				Scenario 2					Scenario 3						
Instance	*EC*	*WC*	*TC*	*#R*	*EC*	*WC*	*TC*	*#R*	*t (sec)*	*EC*	*WC*	*TC*	*#R*	*t (sec)*	$\%\Delta^{1-2}$	$\%\Delta^{1-3}$
c101c5-s3	257.8	807.1	1064.9	3	257.8	807.1	1064.9	3	0.3	257.8	736.6	**994.3**	3	0.4	0.0	6.6
c103c5-s2	175.4	530.2	705.6	3	*176.1*	514.7	**690.8**	4	0.11	*176.1*	480.5	**656.6**	4	0.2	2.1	6.9
c206c5-s4	242.6	763.9	1006.4	3	*252.1*	739.5	**991.6**	4	0.4	*249.8*	710.2	**960.0**	4	0.2	1.5	4.6
c208c5-s3	164.3	499.1	663.5	2	164.3	499.1	663.5	2	0.3	164.3	462.6	**626.9**	2	0.3	0.0	5.5
r104c5-s3	136.7	440.7	577.4	1	*137.0*	427.0	**564.0**	1	0.5	*137.2*	389.3	**526.5**	2	0.4	2.3	8.8
r105c5-s3	156.1	486.4	642.4	2	156.1	486.4	642.4	2	0.3	*156.3*	447.3	**603.6**	3	0.2	0.0	6.1
r202c5-s3	128.9	388.9	517.8	2	128.9	388.9	517.8	2	0.8	128.9	388.4	**517.3**	2	0.6	0.0	0.1
r203c5-s4	179.1	534.3	713.4	3	179.1	534.3	713.4	3	0.5	179.1	517.6	**696.7**	3	0.5	0.0	2.3
rc105c5-s4	233.8	751.4	985.2	3	*233.8*	745.1	**978.9**	4	0.2	*247.5*	667.1	**914.7**	5	0.3	0.6	7.2
rc108c5-s4	253.9	766.1	1020.0	3	253.9	766.1	1020.0	3	0.6	253.9	710.7	**964.6**	3	0.3	0.0	5.4
rc204c5-s4	185.2	558.9	744.1	2	*185.4*	537.6	**723.0**	3	3.7	*185.4*	528.2	**713.7**	3	2.5	2.8	4.1
rc208c5-s3	168.0	525.6	693.6	2	168.0	525.6	693.6	2	1.3	168.0	488.7	**656.7**	2	1.0	0.0	5.3
Average	190.1	587.7	777.8	2.4	191.0	580.9	772.0	2.8	0.7	192.0	543.9	736.0	3.0	0.6	0.8	5.2

Table 7.3. Results for 10-customer instances

	Scenario 1				Scenario 2					Scenario 3						
Instance	*EC*	*WC*	*TC*	*#R*	*EC*	*WC*	*TC*	*#R*	*t (min)*	*EC*	*WC*	*TC*	*#R*	*t (min)*	$\%\Delta^{1-2}$	$\%\Delta^{1-3}$
c101c10-s5	388.3	1208.5	1596.7	5	*389.8*	1186.9	**1576.6**	5	< 1	*388.6*	1105.8	**1494.5**	6	8	1.3	6.4
c104c10-s4	273.9	842.2	1116.2	3	*276.1*	841.3	1117.4	4	600	*276.1*	795.1	**1071.2**	4	600	-0.1	4.0
c202c10-s5	304.1	884.6	1188.6	5	*304.4*	879.0	**1183.4**	6	< 1	*304.4*	852.9	**1157.3**	6	< 1	0.4	2.6
c205c10-s3	228.3	691.8	920.1	2	*228.9*	685.9	**914.8**	3	< 1	*232.6*	652.1	**884.7**	4	3	0.6	3.8
r102c10-s4	249.2	812.1	1061.3	3	249.2	812.1	1061.3	3	< 1	249.2	770.3	**1019.4**	3	< 1	0.0	3.9
r103c10-s3	206.3	639.1	845.4	3	206.3	639.1	845.4	3	86	*210.9*	593.1	**804.0**	4	50	0.0	4.9
r201c10-s4	241.5	733.5	975.1	5	241.5	733.5	975.1	5	< 1	*241.6*	700.5	**942.1**	6	< 1	0.0	3.4
r203c10-s5	222.6	650.4	873.1	4	222.6	650.4	873.1	4	600	222.6	648.9	**871.5**	4	600	0.0	0.2
rc102c10-s4	423.5	1300.8	1724.4	3	423.5	1300.8	1724.4	3	< 1	423.5	1245.8	**1669.3**	3	< 1	0.0	3.2
rc108c10-s4	347.9	1054.7	1402.6	3	347.9	1054.7	1402.6	3	49	*352.1*	1002.7	**1354.8**	4	183	0.0	3.4
rc201c10-s4	412.9	1256.9	1669.8	6	*413.5*	1237.9	**1651.4**	7	< 1	*413.5*	1222.3	**1635.8**	7	< 1	1.1	2.0
rc205c10-s4	326.0	1001.5	1327.4	3	326.0	1001.5	1327.4	3	25	*333.0*	961.8	**1294.8**	4	110	0.0	2.5
Average	302.0	923.0	1225.0	3.8	302.5	918.6	1221.1	4.1	272.0	304.0	879.3	1183.3	4.6	222.0	0.3	3.4

Table 7.4. Results for 15-customer instances

	Scenario 1				Scenario 2					Scenario 3						
Instance	*EC*	*WC*	*TC*	*#R*	*EC*	*WC*	*TC*	*#R*	*Gap*	*EC*	*WC*	*TC*	*#R*	*Gap*	$\%\Delta^{1-2}$	$\%\Delta^{1-3}$
c103c15-s5	348.5	1065.8	1414.3	5	*447.9*	1357.4	1805.3	6	57.3	*350.4*	999.7	**1350.1**	6	100.0	-27.6	4.5
c106c15-s3	275.1	885.4	1160.5	2	275.1	885.4	1160.5	2	44.6	*339.9*	960.8	1300.7	4	100.0	0.0	-12.1
c202c15-s5	383.6	1133.5	1517.1	5	*425.5*	1281.0	1706.4	6	69.9	*391.7*	1111.8	**1503.5**	6	100.0	-12.5	0.9
c208c15-s4	300.6	923.3	1223.8	3	*301.8*	921.7	**1223.6**	3	58.0	*301.8*	873.8	**1175.6**	3	100.0	0.0	3.9
r102c15-s8	412.8	1291.3	1704.1	6	*421.3*	1287.6	1708.9	6	33.8	*413.3*	1184.8	**1598.1**	7	97.0	-0.3	6.2
r105c15-s6	336.2	1046.7	1382.8	4	*337.4*	1033.6	**1371.0**	5	55.5	*337.4*	947.7	**1285.0**	5	64.1	0.9	7.1
r202c15-s6	507.3	1507.2	2014.6	10	No solution					No solution						
r209c15-s5	313.2	930.7	1244.0	6	*325.9*	955.7	1281.6	7	84.3	*358.0*	1060.0	1418.0	7	100.0	-3.0	-14.0
rc103c15-s5	397.7	1255.1	1652.8	4	*399.4*	1231.7	**1631.1**	5	37.1	*400.2*	1089.7	**1489.9**	6	100.0	1.3	9.9
rc108c15-s5	370.3	1183.8	1554.0	4	*378.5*	1162.6	**1541.1**	4	50.0	*370.4*	1073.8	**1444.1**	5	100.0	0.8	7.1
rc202c15-s5	394.4	1222.0	1616.4	6	*401.6*	1212.5	**1614.1**	7	68.1	*466.2*	1331.9	1798.1	7	100.0	0.1	-11.2
rc204c15-s7	382.2	1094.4	1476.6	7	*431.5*	1216.7	1648.2	8	84.3	*464.8*	1271.2	1736.0	10	100.0	-11.6	-17.6
Average	368.5	1128.3	1496.7	5.2	376.9	1140.5	1517.4	5.4	58.4	381.3	1082.3	1463.6	6.0	96.5	-4.7	-1.4

8. CONCLUSION

In this thesis, the influence of battery degradation on the route and charge schedules of the EVs was investigated within the contexts of the ETSPTW and EVRPTW. In Chapter 4, we extended the ETSPTW by incorporating battery wear cost and proposed a mathematical model.

In Chapter 5, we developed a matheuristic algorithm, MatHeur, which is a VNS-based method enhanced with an exact solver employed for making recharge-related decisions. We extended the mathematical model of the FRVCP by considering battery degradation, and solving it on CPLEX requires a reasonably short runtime. We also developed a new mechanism, *Slack*, that is considered during the construction and local search stages for the insertion of charging stations in the next phase.

The performance of MatHeur was validated using benchmark instances from the literature in Chapter 6. MatHeur outperformed CPLEX in terms of solution quality and computational time in the small-size instances. Since no benchmark results are provided in the literature regarding our problem, we made comparisons among the solutions obtained with MatHeur by aiming the minimization of distance and of operational costs including battery wear cost, respectively. Our results revealed that an average of 5% cost-saving is attainable when battery degradation is considered while making routing and charging decisions. Furthermore, we obtained the tours that have more frequent stops for recharging en route. Thus, we demonstrated the utility of considering battery degradation during the route and charge planning. We also analyzed how much our solutions are sensitive with respect to battery size of the EV and time windows restrictions, and we observed that (i) the tours with fewer stops for recharging and less operational costs are obtained as the battery capacity increases; and (ii) the recharge frequency does not change

significantly in the presence of time windows whereas the cost of the tour reduces as the time window restrictions relax. Finally, we demonstrated that the multi-start version of MatHeur reaches better convergence while the runtime increases significantly.

In Chapter 7, we solved the mathematical model of the EVRPTW-BD for the small-size instances from the literature. The results showed that the EVs may travel longer distances due to more frequent recharging, hence, consume more energy. However, the increased energy cost is offset in the total operational costs since the wear cost is considerably higher compared to the energy cost. Moreover, optimizing overnight charging at the depot can bring additional cost savings as opposed to full charge, which is a common assumption in the literature and practice in the sector. Although our experiments involved only small-size instances, we observed excessive computational times in some instances, which could not be solved to optimality.

Future research may focus on developing solution approaches that provide high-quality solutions for large-size problems of the EVRPTW-BD with reasonable computational effort. Moreover, integrating non-increasing and custom wear cost functions into mathematical models might also be another future research direction. Finally, the impact of charging speed, such as normal, fast and super-fast, on the battery wear can be investigated and integrated into our problem.

Appendix A. Data Modification

Integer distances in a distance matrix mainly result in the violation of triangular inequality and overestimation of the results. Therefore, we calculate the Euclidean distances in two decimals. However, the tour lengths are increased with the elimination of overestimation. Hence, we extend the length of the planning horizon and late arrival time of customer nodes in the problem instances.

Table A.1. Extension of late arrival times in the small-size problem instances

Instance	Integer BKS	2-Decimal BF	%Δ	Increase in TW
n20w120.1	267	280.74	5.15	6%
n20w120.2	218	225.92	3.63	4%
n20w120.3	303	310.25	2.39	3%
n20w120.4	300	309.33	3.11	4%
n20w120.5	240	246.61	2.75	3%
n20w140.1	176	184.94	5.08	6%
n20w140.2	272	280.31	3.06	4%
n20w140.3	236	241.97	2.53	3%
n20w140.4	255	258.54	1.39	2%
n20w140.5	225	228.52	1.56	2%
n20w160.1	241	250.82	4.07	5%
n20w160.2	201	207.77	3.37	4%
n20w160.3	201	206.62	2.80	3%
n20w160.4	203	209.21	3.06	4%
n20w160.5	245	252.93	3.24	4%
n20w180.1	253	260.47	2.95	3%
n20w180.2	265	273.93	3.37	4%
n20w180.3	271	278.87	2.90	3%
n20w180.4	201	218.22	8.57	9%
n20w180.5	193	199.04	3.13	4%
n20w200.1	233	239.74	2.89	3%
n20w200.2	203	208.25	2.59	3%
n20w200.3	249	257.04	3.23	4%
n20w200.4	293	297.85	1.66	2%
n20w200.5	227	231.59	2.02	3%

Table A.1 and Table A.2 report the increase in the TSPTW tour lengths when the Euclidean distances are truncated in two decimal places instead of rounded down to the nearest integer. The first column shows the nomenclature of the instances. The column under ‘Integer BKS’ shows the length of the TSPTW tour of the optimal or the BKS in the literature. We report the length of our best-found (BF) TSPTW tour under column ‘2-Decimal BF’ when the Euclidean distances have two decimal places. The increase rate in

the length of the tours is reported under column '%Δ'. In the last column, we round up the values reported under '%Δ'.

Table A.2. Extension of late arrival times in the large-size problem instances

Instance	Integer BKS	2-Decimal BF	%Δ	Increase in TW
n150w120.1	734	786.51	7.15	8%
n150w120.2	677	727.89	7.52	8%
n150w120.3	747	787.96	5.48	6%
n150w120.4	763	812.89	6.54	7%
n150w120.5	689	734.42	6.59	7%
n150w140.1	762	811.4	6.48	7%
n150w140.2	755	807.72	6.98	7%
n150w140.3	613	670.93	9.45	10%
n150w140.4	676	717.49	6.14	7%
n150w140.5	663	709.88	7.07	8%
n150w160.1	706	752.93	6.65	7%
n150w160.2	711	756.38	6.38	7%
n150w160.3	608	659.79	8.52	9%
n150w160.4	672	712.69	6.06	7%
n150w160.5	658	705.56	7.23	8%
n200w120.1	799	918.05	14.90	15%
n200w120.2	721	774.13	7.37	8%
n200w120.3	880	939.96	6.81	7%
n200w120.4	777	836.96	7.72	8%
n200w120.5	841	905.15	7.63	8%
n200w140.1	834	904.68	8.47	9%
n200w140.2	760	819.19	7.79	8%
n200w140.3	758	821.27	8.35	9%
n200w140.4	816	903.21	10.69	11%
n200w140.5	822	882.23	7.33	8%

The late arrival time of each node in the problem instances increased by a fixed amount which is calculated by multiplying the length of the planning horizon in the instance with the increase rate reported under the last column.

Appendix B. Comparison of Single- and Multi-Start Approaches

In this appendix, we present the detailed comparative results obtained by single- and multi-start version of MatHeur. Table B.1 and Table B.2 display the results for the instances with 5- and 10-stations, respectively.

Table B.1. Comparison of single- and multi-start results on large-size instances with 5-station

	Single-start				Multi-start			
Instance	Best	Avg	%Dev	t (s)	Best	Avg	%Dev	t (s)
n150w120s5.1	2946.55	3026.92	2.73	31.00	2965.17	3016.66	1.74	123.60
n150w120s5.2	2519.96	2580.61	2.41	39.12	2525.89	2548.67	0.90	139.00
n150w120s5.3	3176.46	3180.66	0.13	19.44	3083.72	3157.64	2.40	81.10
n150w120s5.4	2704.49	2740.96	1.35	29.20	2695.91	2729.14	1.23	83.40
n150w120s5.5	2763.56	2799.74	1.31	40.84	2776.84	2787.87	0.40	137.50
n150w140s5.1	2917.76	2958.63	1.40	41.00	2917.76	2928.39	0.36	122.70
n150w140s5.2	2986.75	3093.56	3.58	37.64	2984.41	3018.23	1.13	133.70
n150w140s5.3	2434.18	2481.00	1.92	39.56	2423.65	2452.80	1.20	124.70
n150w140s5.4	2630.78	2674.19	1.65	25.40	2630.39	2633.44	0.12	97.20
n150w140s5.5	2545.28	2609.29	2.51	38.16	2533.40	2581.29	1.89	133.70
n150w160s5.1	2819.10	2897.34	2.78	27.84	2804.85	2851.14	1.65	90.60
n150w160s5.2	2832.41	2954.21	4.30	41.20	2832.56	2878.97	1.64	117.10
n150w160s5.3	2376.24	2399.40	0.97	25.84	2368.67	2378.95	0.43	93.80
n150w160s5.4	2700.12	2786.16	3.19	25.48	2772.13	2797.98	0.93	85.10
n150w160s5.5	2629.97	2716.95	3.31	43.44	2620.69	2670.50	1.90	129.70
n200w120s5.1	2882.18	3048.46	5.77	94.40	2863.59	2942.53	2.76	284.30
n200w120s5.2	2894.23	2951.86	1.99	72.08	2892.44	2922.91	1.05	232.00
n200w120s5.3	3282.02	3351.77	2.13	78.64	3275.83	3314.14	1.17	265.70
n200w120s5.4	3234.27	3276.80	1.32	65.76	3224.07	3252.10	0.87	248.00
n200w120s5.5	3135.87	3177.92	1.34	71.36	3135.87	3159.71	0.76	273.80
n200w140s5.1	3146.56	3274.68	4.07	102.96	3154.12	3215.69	1.95	319.00
n200w140s5.2	3121.76	3257.40	4.34	96.44	3138.26	3170.65	1.03	290.10
n200w140s5.3	2852.66	3025.34	6.05	63.40	2899.02	2945.99	1.62	214.30
n200w140s5.4	2977.19	3108.29	4.40	107.20	2977.19	3056.00	2.65	288.20
n200w140s5.5	3204.75	3279.94	2.35	73.68	3219.15	3255.69	1.14	256.50
Average	2868.60	2946.08	2.69	53.24	2868.62	2906.68	1.32	174.59

Table B.2. Comparison of single- and multi-start results on large-size instances with 10-station

	Single-start				Multi-start			
Instance	Cost	Avg	%Dev	t (s)	Cost	Avg	%Dev	t (s)
n150w120s10.1	2882.64	2944.86	2.16	34.68	2882.27	2931.32	1.70	135.00
n150w120s10.2	2472.51	2518.49	1.86	39.00	2479.22	2490.36	0.45	140.70
n150w120s10.3	3156.89	3160.53	0.12	21.16	3033.24	3105.52	2.38	87.90
n150w120s10.4	2632.86	2670.27	1.42	30.40	2632.59	2646.87	0.54	86.00
n150w120s10.5	2635.41	2680.74	1.72	41.12	2635.83	2657.99	0.84	146.30
n150w140s10.1	2845.26	2902.06	2.00	41.24	2845.26	2869.20	0.84	123.80
n150w140s10.2	2917.03	3023.11	3.64	37.72	2913.75	2941.71	0.96	127.40
n150w140s10.3	2403.06	2441.31	1.59	50.88	2393.46	2417.40	1.00	162.70
n150w140s10.4	2580.90	2612.30	1.22	23.00	2580.90	2581.16	0.01	85.90
n150w140s10.5	2474.20	2532.33	2.35	37.96	2473.78	2501.02	1.10	131.00
n150w160s10.1	2749.64	2831.48	2.98	36.04	2735.39	2781.25	1.68	125.70
n150w160s10.2	2739.07	2896.63	5.75	41.24	2724.41	2830.14	3.88	124.20
n150w160s10.3	2317.31	2339.08	0.94	26.84	2317.49	2327.10	0.41	95.70
n150w160s10.4	2648.12	2740.29	3.48	25.00	2704.92	2768.50	2.35	84.80
n150w160s10.5	2564.83	2670.26	4.11	46.96	2573.72	2618.95	1.76	133.00
n200w120s10.1	2822.28	2978.23	5.53	94.00	2809.53	2873.27	2.27	285.10
n200w120s10.2	2831.05	2884.23	1.88	73.56	2829.45	2853.99	0.87	236.00
n200w120s10.3	3184.87	3283.37	3.09	79.24	3184.87	3235.03	1.57	271.10
n200w120s10.4	3126.69	3165.90	1.25	64.04	3127.11	3148.50	0.68	240.30
n200w120s10.5	3052.36	3077.98	0.84	58.08	3052.36	3061.83	0.31	214.10
n200w140s10.1	3094.30	3240.56	4.73	102.36	3097.50	3158.51	1.97	314.10
n200w140s10.2	3057.77	3165.09	3.51	99.80	3062.16	3096.14	1.11	303.50
n200w140s10.3	2811.51	2984.60	6.16	66.44	2866.95	2904.45	1.31	233.80
n200w140s10.4	2960.55	3071.69	3.75	112.64	2960.55	3026.64	2.23	295.30
n200w140s10.5	3164.25	3231.49	2.13	75.96	3170.32	3205.88	1.12	259.60
Average	2805.01	2881.88	2.73	54.37	2803.48	2841.31	1.33	177.72

BIBLIOGRAPHY

Almouhanna, A., Quintero-Araujo, C. L., Panadero, J., Juan, A. A., Khosravi, B., and Ouelhadj, D. (2020). The location routing problem using electric vehicles with constrained distance. *Computers & Operations Research, 115*. doi: 10.1016/j.cor.2019.104864

Barco, J., Guerra, A., Muñoz, L., and Quijano, N. (2017). Optimal routing and scheduling of charge for electric vehicles: A case study. *Mathematical Problems in Engineering*. doi: 10.1155/2017/8509783

Barré, A., Deguilhem, B., Grolleau, S., Gérard, M., Suard, F., and Riu, D. (2013). A review on lithium-ion battery ageing mechanisms and estimations for automotive applications. *Journal of Power Sources, 241*, 680–689. doi: 10.1016/j.jpowsour.2013.05.040

Bruglieri, M., Mancini, S., Pezzella, F., and Pisacane, O. (2016). A new mathematical programming model for the green vehicle routing problem. *Electronic Notes in Discrete Mathematics, 55*, 89-92. doi: 10.1016/j.endm.2016.10.023

Çatay, B. and Keskin, M. (2017). The impact of quick charging stations on the route planning of electric vehicles. *IEEE Symposium on Computers and Communications (ISCC)*, 152-157. doi: 10.1109/ISCC.2017.8024521

da Silva, R., F., and Urrutia, S. (2010). A general VNS heuristic for the traveling salesman problem with time windows. *Discrete Optimization, 7* (4), 203-211. doi: 10.1016/j.disopt.2010.04.002

Deutsch, Y., and Golany, B. (2018). A parcel locker network as a solution to the logistics last mile problem. *International Journal of Production Research, 56*, 251-261, doi: 10.1080/00207543.2017.1395490

Doppstadt, C., Koberstein, A., and Vigo, D. (2016). The hybrid electric vehicle traveling salesman problem. *European Journal of Operational Research, 253* (3), 825-842. doi: 10.1016/j.ejor.2016.03.006

Doppstadt, C., Koberstein, A., and Vigo, D. (2020). the hybrid electric vehicle traveling salesman problem with time windows. *European Journal of Operational Research,*

284 (2), 675-692. doi: 10.1016/j.ejor.2019.12.031

Erdelić, T., and Carić, T. (2019). A survey on the electric vehicle routing problem: variants and solution approaches. *Journal of Advanced Transportation, 2019*. doi: 10.1155/2019/5075671

Erdoğan S., and Miller-Hooks, E. (2012). A green vehicle routing problem. *Transportation Research Part E: Logistics and Transportation Review, 48* (1), 100-114. doi: 10.1016/j.tre.2011.08.001

Felipe, Á., Ortuño, M. T., Righini, G., and Tirado, G. (2014). A heuristic approach for the green vehicle routing problem with multiple technologies and partial recharges. *Transportation Research Part E: Logistics and Transportation Review, 71*, 111-128. doi: 10.1016/j.tre.2014.09.003

Feng, W., and Figliozzi, M. (2013). An economic and technological analysis of the key fac-tors affecting the competitiveness of electric commercial vehicles: A case study from the USA market. *Transportation Research Part C: Emerging Technologies, 26*, 135-145. doi: 10.1016/j.trc.2012.06.007

Fleming, C. L., Griffis, S. E., and Bell, J. E. (2013). The effects of triangle inequality on the vehicle routing problem. *European Journal of Operational Research, 224* (1), 1-7. doi: 10.1016/j.ejor.2012.07.005

Fries, M., Kerler, M., Rohr, S. and Sinning M. (2017). An overview of costs for vehicle components, fuels, greenhouse gas emissions and total cost of ownership - Update 2017. doi: 10.13140/RG.2.2.11685.40164

Gendreau, M., Hertz, A., Laporte, G., and Stan, M. (1998). A generalized insertion heuristic for the traveling salesman problem with time windows. *Operations Research, 46* (3), 330-335. doi: 10.1287/opre.46.3.330

Goeke, D., and Schneider, M. (2015). Routing a mixed fleet of electric and conventional vehicles. *European Journal of Operational Research, 245* (1), 81-99. doi: 10.1016/j.ejor.2015.01.049

Guo, F., Zhang, J., Huang, Z., and Huang, W. (2022). Simultaneous charging station location-routing problem for electric vehicles: Effect of nonlinear partial charging and battery degradation. *Energy, 250*. doi: 10.1016/j.energy.2022.123724

Han, S., Han, S., and Aki, H. (2014). A practical battery wear model for electric vehicle charging applications. *Applied Energy*, *113*, 1100–1108. doi: 10.1016/j.apenergy.2013.08.062

Hansen, P., Mladenović, N., Brimberg, J., and Peréz, A. M. (2010). Variable neighborhood search. In Gendreau, M., and Potvin, J. Y. (Eds.). (2010). *Handbook of metaheuristics* (pp. 61-86). New York: Springer. doi: 10.1007/978-1-4419-1665-5

Hof, J., Schneider, M., and Goeke, D. (2017). Solving the battery swap station location-routing problem with capacitated electric vehicles using an AVNS algorithm for vehicle-routing problems with intermediate stops. *Transportation Research Part B: Methodological*, *97*, 102-112. doi: 10.1016/j.trb.2016.11.009

International Energy Agency (2020). CO2 emissions by sector, world 1990-2018. Retrieved from https://www.iea.org/data-and-statistics?country=WORLD&fuel=CO2%20emissions&indicator=CO2BySector

International Energy Agency. (2020). CO2 emissions from fuel combustion: Overview. Retrieved from https://www.iea.org/reports/co2-emissions-from-fuel-combustion-overview#data-service

Jiang, L., Chang, H., Zhao, S., Dong, J., and Lu, W. (2019). A travelling salesman problem with carbon emission reduction in the last mile delivery. *IEEE Access*, *7*, 61620-61627. doi: 10.1109/ACCESS.2019.2915634

Kancharla, S. R., and Ramadurai, G. (2020). Electric vehicle routing problem with non-linear charging and load-dependent discharging. *Expert Systems with Applications*, *160*. doi: 10.1016/j.eswa.2020.113714

Keskin, M., and Çatay, B. (2016). Partial recharge strategies for the electric vehicle routing problem with time windows. *Transportation Research Part C: Emerging Technologies*, *65*, 111-127. doi: 10.1016/j.trc.2016.01.013

Keskin, M., and Çatay, B. (2018). A matheuristic method for the electric vehicle routing problem with time windows and fast chargers. *Computers & Operations Research*, *100*, 172-188. doi: 10.1016/j.cor.2018.06.019

Keskin, M., Çatay, B., and Laporte, G. (2021). A simulation-based heuristic for the

electric vehicle routing problem with time windows and stochastic waiting times at recharging stations. *Computers & Operations Research*, *125*. doi: 10.1016/j.cor.2020.105060

Keskin, M., Laporte, G., and Çatay, B. (2019). Electric vehicle routing problem with time-dependent waiting times at recharging stations. *Computers & Operations Research, 107*, 77-94. Doi: doi.org/10.1016/j.cor.2019.02.014

Küçükoğlu, İ., Dewil, R., and Cattrysse, D. (2019). Hybrid simulated annealing and tabu search method for the electric travelling salesman problem with time windows and mixed charging rates. *Expert Systems with Applications, 134*, 279-303. doi: 10.1016/j.eswa.2019.05.037

Kucukoglu, I., Dewil, R., and Cattrysse, D. (2021). The electric vehicle routing problem and its variations: A literature review. *Computers & Industrial Engineering*, *161*. doi: 10.1016/j.cie.2021.107650

Lin, B., Ghaddar, B., and Nathwani, J. (2021). Electric vehicle routing with charging/discharging under time-variant electricity prices. *Transportation Research Part C: Emerging Technologies, 130*. doi: 10.1016/j.trc.2021.103285

Lu, J., Chen, Y., Hao, J. K., and He, R. (2020). The time-dependent electric vehicle routing problem: Model and solution. *Expert Systems with Applications, 161*. doi: 10.1016/j.eswa.2020.113593

McKinsey&Company (2016). Parcel delivery: The future of last mile. Retrieved from https://www.mckinsey.com/~/media/mckinsey/industries/travel%20transport%20and%20logis-tics/our%20insights/how%20customer%20demands%20are%20reshaping%20last%20mile%20delivery/parcel_delivery_the_future_of_last_mile.ashx

Mladenović, N., and Hansen, P. (1997). Variable neighborhood search. *Computers & Operations Research*, *24* (11), 1097–1100. doi:10.1016/s0305-0548(97)00031-2

Mladenović, N., Todosijević, R., & Urošević, D. (2012). An efficient GVNS for solving traveling salesman problem with time windows. *Electronic Notes in Discrete Mathematics*, 39, 83–90. doi: 10.1016/j.endm.2012.10.012

Montoya, A., Guéret, C., Mendoza, J. E., & Villegas, J. G. (2017). The electric vehicle

routing problem with nonlinear charging function. *Transportation Research Part B: Methodological, 103,* 87-110. doi: 10.1016/j.trb.2017.02.004

Nykvist, B., Sprei, F., and Nilsson, M. (2019). Assessing the progress toward lower priced long range battery electric vehicles. *Energy Policy, 124,* 144–155. doi:10.1016/j.enpol.2018.09.035

Ohlmann, J., W., and Thomas, B., W. (2007). A compressed-annealing heuristic for the traveling salesman problem with time windows. *INFORMS Journal on Computing, 19* (1), 80-90. doi: 10.1287/ijoc.1050.0145

Pelletier, S., Jabali, O., and Laporte, G. (2016). 50th anniversary invited article - goods distribution with electric vehicles: review and research perspectives. *Transportation Science, 50* (1), 3–22. doi: 10.1287/trsc.2015.0646

Pelletier, S., Jabali, O., and Laporte, G. (2018). Charge scheduling for electric freight vehicles. *Transportation Research Part B: Methodological, 115,* 246-269. doi: 10.1016/j.trb.2018.07.010

Pelletier, S., Jabali, O., Laporte, G., and Veneroni, M. (2017). Battery degradation and behaviour for electric vehicles: Review and numerical analyses of several models. *Transportation Research Part B: Methodological, 103,* 158–187. doi: 10.1016/j.trb.2017.01.020

Rastani, S., amd Çatay, B. (2021). A large neighborhood search-based matheuristic for the load-dependent electric vehicle routing problem with time windows. *Annals of Operations Research*, 1-33. doi: doi.org/10.1007/s10479-021-04320-9

Rastani, S., Yüksel, T., and Çatay, B. (2019). Effects of ambient temperature on the route planning of electric freight vehicles. *Transportation Research Part D: Transport and Environment, 74,* 124-141. doi: 10.1016/j.trd.2019.07.025

Roberti, R., and Wen, M. (2016). The Electric Traveling Salesman Problem with Time Windows. *Transportation Research Part E: Logistics and Transportation Review, 89,* 32-52. doi: 10.1016/j.tre.2016.01.010

Rohrbeck, B., Berthold, K., and Hettich, F. (2018). Location planning of charging stations for electric city buses considering battery ageing effects. *Operations Research Proceedings*, 701-707. doi: 10.1007/978-3-319-89920-6_93

Sadati, M. E. H., Akbari, V., and Çatay, B. (2022). Electric vehicle routing problem with flexible deliveries. *International Journal of Production Research*, 1-27. Doi: 10.1080/00207543.2022.2032451

Sadati, M., E., H., and Çatay, B. (2021). A hybrid variable neighborhood search approach for the multi-depot green vehicle routing problem. *Transportation Research Part E: Logistics and Transportation Review*, *149*. doi: 10.1016/j.tre.2021.102293

Sassi, O., Cherif, W. R. and Oulamara, A. (2014). Vehicle routing problem with mixed fleet of conventional and heterogenous electric vehicles and time dependent charging costs. *Technical Report*. Retrieved from: https://hal.archives-ouvertes.fr/hal-01083966/document

Schiffer, M., and Walther, G. (2017). The electric location routing problem with time windows and partial recharging. *European Journal of Operational Research, 260* (3), 995-1013. doi: 10.1016/j.ejor.2017.01.011

Schiffer, M., Klein, P. S., Laporte, G., and Walther, G. (2021). Integrated planning for electric commercial vehicle fleets: A case study for retail mid-haul logistics networks. *European Journal of Operational Research*, *291* (3), 944-960. doi: 10.1016/j.ejor.2020.09.054

Schiffer, M., Stütz, S., and G.Walther, (2016). Are ECVs breaking even?: Competitiveness of electric commercial vehicles in retail logistics. Retrieved from https://www.om.rwth-aachen.de/data/uploads/om-022016.pdf

Schneider, M., Stenger, A., and Goeke, D. (2014). The electric vehicle-routing problem with time windows and recharging stations. *Transportation Science*, *48* (4), 500-520. doi: 10.1287/trsc.2013.0490

Schneider, M., Stenger, A., and Hof, J. (2015). An adaptive VNS algorithm for vehicle routing problems with intermediate stops. *OR Spectrum*, *37*, 353–387. doi: 10.1007/s00291-014-0376-5

Solomon, M. M. (1987). Algorithms for the Vehicle routing and scheduling problems with time window constraints. *Operations Research*, *35* (2), 254-265

Suzuki, Y. (2014). A variable-reduction technique for the fixed-route vehicle-refueling problem. *Computers & Industrial Engineering*, *67*, 204-215. doi:

10.1016/j.cie.2013.11.007

Taş, D. (2021). Electric vehicle routing with flexible time windows: a column generation solution approach. *Transportation Letters*, *13* (2), 97-103. doi: 10.1080/19427867.2020.1711581

U.S Energy Information Administration (EIA). (2020). Table 5.3. Average price of electricity to ultimate customers. Retrieved from https://www.eia.gov/electricity/monthly/epm_table_grapher.php?t=epmt_5_03

Wang, J., Kang. L., and Liu, Y. (2020). Optimal scheduling for electric bus fleets based on dynamic programming approach by considering battery capacity fade. *Renewable and Sustainable Energy Reviews, 130*. doi: 10.1016/j.rser.2020.109978

Wang, L., Gao, S., Wang, K., Li, T., Li, L., and Chen, Z. (2020). Time-dependent electric vehicle routing problem with time windows and path flexibility. *Journal of Advanced Transportation, 2020*. doi: 10.1155/2020/3030197

Wolff, S., Seidenfus, M., Gordon, K., Álvarez, S., Kalt, S., and Lienkamp, M. (2020). Scalable life-cycle inventory for heavy-duty vehicle production. *Sustainability*, *12* (13), 5396. doi:10.3390/su12135396

Xu, M., Wu, T. and Tan, Z. (2021). Electric vehicle fleet size for carsharing services considering on-demand charging strategy and battery degradation. *Transportation Research Part C: Emerging Technologies*, *127*. doi: 10.1016/j.trc.2021.103146

Yang, J., and Sun, H. (2015). Battery swap station location-routing problem with capacitated electric vehicles. *Computers & Operations Research*, *55*, 217-232. doi: 10.1016/j.cor.2014.07.003

Zang, Y., Wang, M. and Qi, H. (2022). A column generation tailored to electric vehicle routing problem with nonlinear battery depreciation. *Computers & Operations Research*, 13. doi: 10.1016/j.cor.2021.105527

Zhang, L., Zeng, Z. and Qu, X. (2021). On the role of battery capacity fading mechanism in the lifecycle cost of electric bus fleet. *IEEE Transactions on Intelligent Transportation Systems*, *22* (4), 2371-2380. doi: 10.1109/TITS.2020.3014097

Zhu, X., Yan, R., Huang, Z., Wei, W., Yang, J., and Kudratova, S. (2020). Logistic optimization for multi depots loading capacitated electric vehicle routing problem

from low carbon perspective. *IEEE Access*, *8*, 31934-31947. doi: 10.1109/ACCESS.2020.2971220